

Original Article

Cite this article: Breckenridge J, Maravelis AG, Catuneanu O, Ruming K, Holmes E, and Collins WJ (2019) Outcrop analysis and facies model of an Upper Permian tidally influenced fluvio-deltaic system: Northern Sydney Basin, SE Australia. *Geological Magazine* **156**: 1715–1741. <https://doi.org/10.1017/S0016756818000973>

Received: 5 November 2017

Revised: 21 November 2018

Accepted: 17 December 2018

First published online: 7 March 2019

Keywords:

deltas; facies analysis; Late Permian; Northern Sydney Basin; sequence stratigraphy; tidal reworking

Author for correspondence:

Angelos G. Maravelis,
Email: angmar@upatras.gr

Outcrop analysis and facies model of an Upper Permian tidally influenced fluvio-deltaic system: Northern Sydney Basin, SE Australia

Jake Breckenridge¹, Angelos G. Maravelis² , Octavian Catuneanu³, Kevin Ruming⁴, Erin Holmes⁴ and William J. Collins⁵

¹School of Environmental and Life Sciences, University of Newcastle, Callaghan, New South Wales 2308, Australia; ²Laboratory of Sedimentology, Department of Geology, University of Patras, Rion 26504, Greece;

³Department of Earth and Atmospheric Sciences, University of Alberta, 1-26 Earth Sciences Building, Edmonton, Alberta T6G 2E3, Canada; ⁴Geological Survey of New South Wales, Division of Resources and Energy, Department of Industry, Maitland, New South Wales 2320, Australia and ⁵The Institute for Geoscience Research (TIGeR), Department of Applied Geology, Curtin University, GPO Box U1987, Perth, Western Australia 6845, Australia

Abstract

An integrated study of sedimentological, sequence-stratigraphic and palaeodispersal analysis was applied to the Upper-Permian clastic sedimentary succession in the Northern Sydney Basin, Australia. The succession is subdivided into fifteen facies and three facies associations. The facies associations are further subdivided into eight sub-facies associations. The sedimentary evolution involves progradation from delta-front to delta-plain to fluvial depositional environments, with a significant increase in sediment grain size across the unconformable contact that separates the deltaic from the overlying fluvial system. In contrast to the delta front that is wave/storm- and/or river-influenced, the delta plain is significantly affected by tides, with the impact of tidal currents decreasing up-sequence in the delta plain. The general lack of wave-influenced sedimentary structures suggests low wave energy in the delta plain. The abrupt termination of the tidal impact in the fluvial realm relates to the steep topographic gradients and high sediment supply, which accompanied the uplift of the New England Orogen. The sequence-stratigraphic framework includes highstand (deltaic forest and topset) and lowstand (fluvial topset) systems tracts, separated by a subaerial unconformity. In contrast to most of the mud-rich modern counterparts, this is an example of a sand-rich tidally influenced deltaic system, developed adjacent to the source region. This investigation presents a depositional model for tidal successions in regions of tectonic uplift and confinement.

1. Introduction

The influence of tides in both recent and ancient deltaic depositional environments has been extensively examined, leading to the development of elegant conceptual models (e.g. Nio & Yang, 1991; Willis, 2005; Martinius & Van den Berg, 2011; Longhitano *et al.* 2012; Plink-Björklund, 2012; Magalhães *et al.* 2014). Despite the confidence provided by sedimentological evidence and facies analysis, the interpretation of deltaic depositional environments is not always straightforward. Tidal influence on sedimentation is common in both estuarine and deltaic environments (Martinius *et al.* 2001; Boyd *et al.* 2006). Similar facies are deposited in both settings but exhibit different architectural styles and facies trends (e.g. retrogradational vs progradational trends, respectively; Legler *et al.* 2013). Tidally influenced deltas have received less attention than the estuarine systems, but some important case studies provided valuable information about their development (e.g. Willis *et al.* 1999; Zeligidis & Kontopoulos, 1999; Mellere & Steel, 2000; Willis & Gabel, 2001; Pontén & Plink-Björklund, 2007; Tänavsuu-Milkeviciene & Plink-Björklund, 2009; Mellere *et al.* 2016; Rossi & Steel, 2016).

Despite the increasing amount of research conducted in ancient examples (Mellere & Steel, 1995; Bhattacharya & Willis, 2001; Martinius *et al.* 2001; Willis, 2005; Pontén & Plink-Björklund, 2009), tidally influenced and tidally dominated deltas are not still widely recognized within the ancient record (Plink-Björklund, 2012). In particular, most of these examples are primarily composed of delta-front deposits, whereas case studies that describe delta-plain deposits are not abundant (e.g. Willis & Gabel, 2003; Rebata *et al.* 2006; Pontén & Plink-Björklund, 2007). Therefore, comprehensive outcrop-based facies models for their development are still needed. Although unembayed shelf-edge tidally influenced deltas have been recorded in the literature (Cummings *et al.* 2006; Carvajal & Steel, 2009; Schwartz & Graham, 2015), they are mostly ascribed to embayment settings on the shelf, most likely as

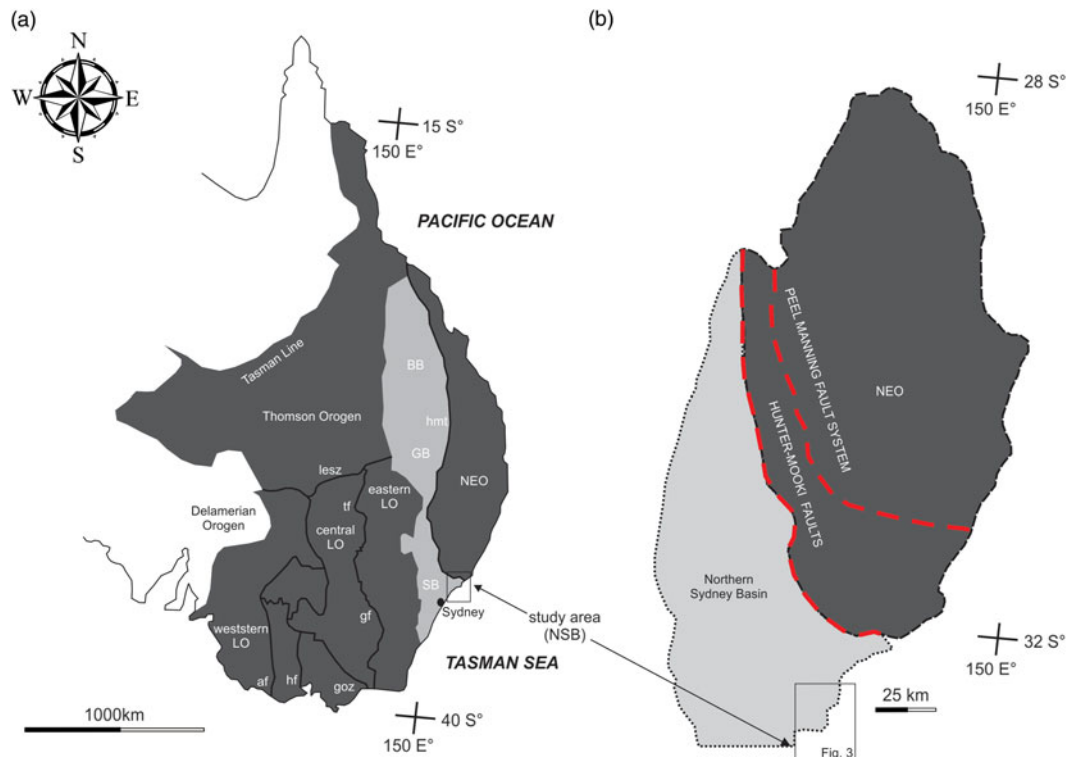


Fig. 1. Geological map of eastern Australia depicting the position of the Sydney Basin with respect to the major structural elements. Abbreviations: LO = Lachlan Orogen; NEO = New England Orogen; GB = Gunnedah Basin; SB = Sydney Basin; BB = Bowen Basin; af = Avoca Fault; goz = Governor Fault; hf = Heathcote Fault Zone; hmt = Hunter-Mooki Trist; gf = Gilmore Fault Zone; lesz = Louth-Eumarrra Shear Zone; tf = Tullamore Fault Zone (from Glen, 2005).

a result of the increased tidal energy in these locations compared to the shelf edge (Porebski & Steel, 2006; Yoshida *et al.* 2007).

Deltas exhibit a complex depositional architecture that depends on the interaction between river input, tidal and wave processes, as well as changes in the prevalence of these competing processes during relative sea-level changes (Willis & Gabel, 2001). These settings are intermittently influenced by tides in an environment mainly dominated by fluvial processes (Plink-Björklund, 2012; Rossi & Steel, 2016). The shift from fluvial to tidal sedimentation has been described in transgressive systems (e.g. Dalrymple *et al.* 1992; Plink-Björklund 2005; Dalrymple & Choi, 2007). Nevertheless, the detailed analysis of facies and facies associations that are involved in this transition in regressive systems needs further investigation. In some of the scarce examples available, this transition occurs gradually with the development of tidally influenced fluvial deposits (Pontén & Plink-Björklund, 2007). In other cases, the change from deltaic to continental sedimentation takes place abruptly, with sudden change from delta-plain to fluvial deposits (Rossi & Steel, 2016).

The Sydney Basin (SB) is a large Permo-Triassic sedimentary depocentre in eastern Australia that rimmed the Gondwanan landmass, contains significant proven coal reserves and offers an opportunity to evaluate important sedimentological and stratigraphic aspects of a tidally influenced fluvio-deltaic system (Fig. 1). The SB and surrounding basins (e.g. Myall Trough) are of great economic importance (e.g. Stewart & Adler, 1995; Alder *et al.* 1998; Montoya, 2012; Maravelis *et al.* 2017a, b; Palozzi *et al.* 2018), and have been the subject of long-standing industry interest. This study focuses on the Upper Permian (PR Warbrooke, unpub. Ph.D thesis, Univ. Newcastle, Australia, 1981; Diessel, 1992; Herbert, 1995) sedimentary succession (*c.* 400 m thick) that outcrops in the Northern Sydney Basin (NSB). The exact age of the Waratah

Sandstone has not been defined, but its stratigraphic position (below the Newcastle Coal Measures) has been documented in exploration wells (Diessel & Warbrooke, 1987). The Upper Permian age of the Newcastle Coal Measures has been documented with high-precision U–Pb chemical abrasion thermal ionization mass spectrometry (CA-TIMS) data (Metcalf *et al.* 2015). The precise documentation of the depositional environments and sub-environments for the strata that make up this succession has received limited attention (PR Warbrooke, unpub. Ph.D thesis, Univ. Newcastle, Australia, 1981; Diessel, 1992), although it is known to contain valuable coal reserves. As a result, the proposed sequence-stratigraphic scenarios are largely lithologically based (Herbert, 1995, 1997) and lack a thorough sedimentological analysis, which is essential for sequence-stratigraphic interpretations. These scenarios suggest a generally regressive sedimentary succession. The current study utilizes more sedimentological data in order to constrain the depositional environments and sub-environments, and the sequence-stratigraphic framework. This basin provides a case study to correlate regressive fluvio-deltaic deposits, over an area of 1800 km².

This research documents a sedimentary succession that encompasses delta-front deposits and the overlying delta-plain facies that are, in turn, capped by fluvial deposits exhibiting a shoaling-upward trend. This study integrates detailed facies analysis, stratigraphic and sequence-stratigraphic correlations, as well as palaeocurrent analysis to unravel the depositional environments, palaeogeographic evolution and sediment palaeodispersal in the NSB. The results of this research will help to better understand the facies and facies associations that occur across the transition zone between the tidal and fluvial sedimentation, providing implications for the nature (gradual vs abrupt) of this transition. Moreover, this analysis provides an example of a regressive

fluvio-deltaic system with sudden temporal changes in the dominant depositional processes, as a result of tectonic uplift and confinement.

2. Geological setting

During the Permian – early Triassic, Australia was part of eastern Gondwana, the southern hemisphere component of supercontinent Pangaea, and was located in high southern palaeolatitudes (Veevers & Powell, 1987). The SB represents the southernmost edge of the larger, N–S-trending, composite Bowen–Gunnedah–Sydney Basin in eastern Australia that is c. 1600 km long (Glen, 2005) (Fig. 1). Stratigraphic equivalents can be traced through Antarctica, South Africa and South America as the foreland basin to the Gondwanide orogen (e.g. Veevers & Powell, 1994). The SB is underlain by two different basement types and displays an asymmetric geometry, with the thickest succession occurring in the northeast. In the southwest, the SB overlies the Early–Middle Palaeozoic Lachlan Orogen, and to the northeast the SB is underlain by the Late Palaeozoic New England Orogen (Roberts & Engel, 1987).

The SB initiated as a continental backarc in the Late Carboniferous – Early Permian (Collins, 1991), confirmed by the trace-element chemistry of gabbroic and basaltic rocks (Jenkins *et al.* 2002). During the later stages of the Early Permian, a mixture of post-rift subsidence and the cessation of loading caused a westward marine transgression over the Lachlan Orogen to the SW during subduction of an east-facing convergent margin in the New England Orogen to the NE (C Danis, unpub. Ph.D thesis, Macquarie Univ., 2012). The NSB experienced subsequent conversion to a foreland basin by progressive west-directed thrusting and folding, as evidenced by the geometry and kinematics of the Late Permian folds and faults in the southern New England Orogen and SB (Collins, 1991; Landenberger *et al.* 1995; Jenkins & Offler, 1996; Glen & Beckett, 1997). The Late Permian deformational pattern in the southern New England Orogen is interpreted as the result of a single but complex compressive tectonic event, the Hunter–Bowen Orogeny, 265–250 Ma ago (Collins, 1991).

The uplifted and over-thrusted New England Orogen became a major sediment contributor into the NSB, and its evolution was responsible for the evolution of the NSB as a foreland basin (Conaghan *et al.* 1982). During the evolution of the SB into a foreland basin, sediments display rapid lateral and vertical facies changes as a result of eustatically and tectonically driven regressions and transgressions (Herbert & Helby, 1980). During the Middle to Late Triassic, the SB was dissected by fold and thrust belts in response to westward-migrating thrust fronts with associated crustal shortening (Glen & Beckett, 1997). This deformation was responsible for the termination of deposition in the SB during the Middle Triassic time (Herbert & Helby, 1980). In this setting, the evolution of the SB is remarkably similar to the evolution of other contemporary sedimentary basins in southern Gondwana, including the Karoo Basin in southern Africa (e.g. Catuneanu *et al.* 1998, 2005; Catuneanu, 2004) and the foreland systems of South America (Menegazzo *et al.* 2016). Similar net progradation of the shoreline has also been documented in the Karoo Basin, although with less evidence for tidal activity (Rubidge *et al.* 2000).

3. Methodology

The reconstruction of palaeodepositional environments and sub-environments through facies analysis is essential for basin analysis and has been applied to non-marine and marine deposits

(Catuneanu & Eriksson, 2002; Catuneanu *et al.* 2006; Maravelis *et al.* 2007; Maravelis & Zeligidis, 2011), and to reveal differences in sedimentary successions between extensional and compressional settings (Di Celma *et al.* 2010; Maravelis *et al.* 2016). In the NSB, the examined lithostratigraphic units include (from oldest to youngest) the Waratah Sandstone and the Lambton, Adamstown and Boolaroo sub-groups. These sub-groups are further subdivided into several formations and members (Fig. 2).

Thirteen outcrops were examined along a 25 km transect of the New South Wales coastline, between Nobbys Head in the north, and Caves Beach in the south (Fig. 3). The size and connectivity of the outcrops varies considerably, with outcrops ranging in size from 40 m long and 10 m high to 1 km long and 120 m high. Most outcrops are several hundreds of metres long and are either connected or partially connected (less than 100 m between outcrops). Only two outcrops are wider-spaced (up to a few km, outcrops 10 and 13). The studied succession encompasses the Waratah Sandstone (outcrop 13) and the Newcastle Coal Measures (outcrops 1–12). Primary sedimentological features (lithology, sedimentary structures and texture) were utilized in order to interpret depositional processes, environments and sub-environments of deposition, and the distribution of architectural elements. The facies analysis was conducted by detailed sedimentological logging, and field photographs. Facies characteristics were used to define facies associations and allow for facies sets to be grouped into ascribed depositional sub-environments. Classification of these sub-environments and their processes allows for an interpretation of the shape and lateral accretion, identifying important architectural elements in the studied succession. Palaeocurrent measurements from sole marks, cross-stratification and clast imbrication revealed the main palaeoflow direction.

Outcrop-based analysis allowed documentation of key stratigraphic surfaces and marker beds in the NSB, which allowed for correlations to be made throughout the studied succession. Coal deposits and volcanoclastic sediments (tuffs) regularly outcrop in the study area and form thick and laterally extensive beds. These deposits were used as marker beds for establishing stronger lithostratigraphic correlations. The upward transitions of depositional environments, documented on stratigraphic columns, revealed the palaeogeographic evolution. The construction of detailed stratigraphic cross-sections assisted in determining the spatial and temporal distribution of the depositional environments and sub-environments. The interpretation of detailed field data, integrated with the identification of sequence-stratigraphic surfaces, led to the proposed sequence-stratigraphic model. This integration of data allowed the documentation of the depositional systems and systems tracts.

4. Sedimentary facies and facies associations

The studied sedimentary succession includes an intricate facies architecture, and 15 depositional facies have been identified (F1–F15). These facies were grouped into three facies associations (FA1–FA3), based on facies assemblages and variations, the dominant depositional process, and the geometry and position of major bounding and stratigraphic surfaces. Furthermore, FA1 and FA2 are subdivided into several sub-facies associations (sub-FA1a and sub-FA1b, and sub-FA2a to sub-FA2f respectively). The main facies characteristics are summarized in Table 1.

4.a. FA1: fluvial deposits

Facies Association 1 (FA1) is over 200 m thick. FA1 includes sedimentological features that are characteristic of a fluvial

Northern Sydney Basin		
Boolaroo sub-group	Fassifern Coal	251 Ma
	Belmont Conglomerate	
	Upper Pilot Coal	
	Mt. Hutton Tuff	
	Mt. Hutton Coal	
	Lower Pilot Coal	
	Hartely Hill Coal	
Adamstown sub-group	Warners Bay Tuff	
	Australasian Coal	
	Charlestown Conglomerate	
	Stockrington Tuff	
	Montrose Coal	
	Whitebridge Conglomerate	
	Wave Hill Tuff	
	Wave Hill Coal	
	Tingira Conglomerate	
	Edgeworth Tuff	
	Upper Fern Valley Coal	
	Redhead Conglomerate	
	Lower Fern Valley Coal	
	Merewether Conglomerate	
	Unnamed Tuff (in Kotara formation)	
Lambton sub-group	Victoria Tunnel Coal	
	Nobbys Tuff	
	Nobbys Coal	
	Signal Hill Member	
	Young Wallsend Coal	
	Cockle Creek Conglomerate Member	
	Yard Coal	
	Ferndale Conglomerate	
	Borehole Coal	
	West Borehole coal	
Tomago Coal Measures	Waratah Sandstone	255 Ma

Fig. 2. Lithostratigraphic chart of the Northern Sydney Basin illustrating the different sub-groups that make up the studied succession (from PR Warbrooke, unpub. Ph.D thesis, Univ. Newcastle, Australia, 1981; Diessel, 1992). The Lambton, Adamstown and Boolaroo sub-groups make up the Newcastle Coal Measures.

depositional environment. These features correspond to depositional elements such as fluvial channels (sub-FA1a) and mid-channel bars deposits (sub-FA1a).

4.a.1. Sub-FA1a: fluvial-dominated channelized deposits

Description:

Sub-FA1a is characterized by thick (2–10 m), stacked sedimentary packages that are dominated by conglomerate and coarse- to medium-grained sandstone (Fig. 4a). Conglomerate in the sub-FA1a is either clast- to matrix-supported (F1) or cross-stratified (F2) (Fig. 4b, c). It is sometimes imbricated (Fig. 4d) and is often overlain by planar and trough cross-bedded conglomerate. The conglomerate is usually structureless, but often displays normal- to reverse-graded units (Fig. 4e). The clasts occur in a sandy matrix, include granules or pebbles (0.2–10 cm), and are sub-rounded to well-rounded. The clasts are composed of sandstone, tuff, mudstone, quartz and chert. Sandstone is often interbedded with conglomerate, it is structureless (F3) at the base of the sandstone beds and may evolve into trough cross-stratified (F4), or planar cross-stratified (F5) and/or compound cross-stratified (F6) towards the top of the beds (Fig. 5a). Trough-cross-stratified sandstone forms both single sets and co-sets that are separated by bounding surfaces, often highlighted by pebbles (Fig. 5b). Compound cross-stratified sandstone forms medium- to thick-bedded (0.2–1 m), stacked sets of both trough- and planar cross-stratified sandstone. In places, the cross-beds display a fining-upward transition from conglomerate to sandstone (Fig. 5c). Ripple cross-laminated sandstone (F7) is present at the top of the beds and is associated with parallel-laminated sandstone (F8, Fig. 5a). Mudstone is rare and restricted in the uppermost parts of these packages. It is interbedded with medium- to thin-bedded sandstone (0.1–0.3 m) and,

when present, it is mostly structureless (F12). Rarely, horizontally laminated mudstone occurs. Transported coal debris and tree branches are common in the sub-FA1a. Very thin (millimetre- to centimetre-thick) mud drapes occur in places in this facies association (Fig. 5d).

The sedimentary packages that make up this sub-FA display a thinning- and fining-upward trend. Thick (2–5 m) conglomeratic bodies dominate the lower parts of these packages and evolve upwards into very thick- (1–2.5 m) to thick-bedded (0.4–0.9 m) sandstone that is interbedded with thinner-bedded conglomerate. These packages evolve upwards into medium- to thin-bedded sandstone (0.1–0.2 m) that is rarely interbedded with thin-bedded (1–5 cm) mudstone (Fig. 5e). They are often arranged into thick (1–5 m) amalgamated units, bounded by erosional surfaces that dip towards the palaeocurrent direction and display a flat to concave-up to erosional pattern (Fig. 4a). These packages pinch out laterally into finer-grained deposits that belong to sub-FA2d (Fig. 5f). The degree of amalgamation is very high and may reach 95% of the sub-FA1a. Rarely, these packages are separated by thin-bedded mudstone. Basal contacts of sub-FA1a with the underlying sediments are often erosional, whereas internally contacts between facies are sharp and/or erosional.

Interpretation:

Sub-FA1 is interpreted as fluvial channels, indicated by the thick sedimentary units that exhibit a general fining-upward trend and concave-up geometry, in association with lack of tidally influenced sedimentary structures. The presence of scarce mud drapes suggests some modification by tidal currents, but they are randomly oriented and thus are probably related to fluvial processes (Rossi & Steel, 2016). This FA contains the coarsest sediments

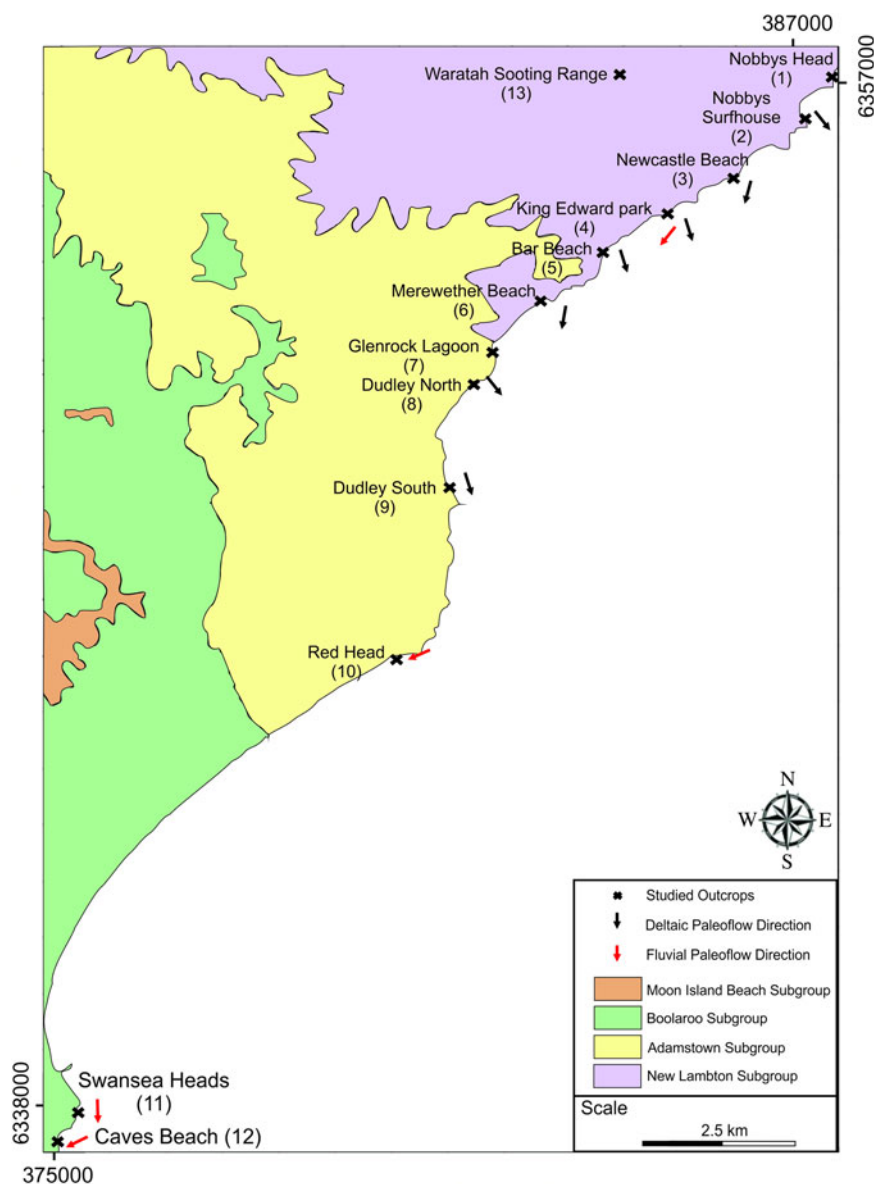


Fig. 3. (Colour online) Map of the Northern Sydney Basin depicting the spatial evolution of the involved sub-groups. Black crosses correspond to the studied sections.

observed within the studied section. The dominance of clast- to matrix-supported (F1) or cross-stratified (F2) conglomerate, and the predominant clast-supported nature of most conglomerates are characteristics of braided stream sediments (Nemec & Steel, 1984). Clast imbrication indicates traction currents during deposition (Whiting *et al.* 1988). Planar and trough cross-stratified conglomerate is ascribed to the migration and deposition of 2D and 3D gravelly dunes respectively (Allen, 1983; Plink-Björklund, 2005). They reflect the deposition of high-energy currents in a channelized environment during lower-flow-regime conditions (Allen, 1983).

Cross-stratified pebbly sandstone indicates migration and deposition of sandy barforms in a fluvial channel and represents downstream accretion under lower-flow-regime conditions (Medici *et al.* 2015). Repeating foresets of conglomerate and sandstone in the cross-beds is ascribed to discharge fluctuations (Steel & Thompson, 1983). Structureless sandstone that is present at the base of channel sandbodies corresponds to deposition during floods (Collinson, 1996). Parallel-laminated sandstone

is developed through migration of bedforms during upper-flow-regime conditions (Collinson, 1996), and cross-laminated sandstone reflects relatively weak currents during the lower-flow regime (Stear, 1978).

The general absence of overbank and floodplain fines (coal and mudstone), in conjunction with the high degree of amalgamation of the sandstone beds, suggests recurrent cut-and-fill processes (Collinson *et al.* 2006). This evidence implies mobile fluvial channels and frequent channel migration that is responsible for the erosion of the associated floodplain deposits (Nichols & Fisher, 2007). Such absence of fine-grained deposits could be associated with recurrent channel avulsion to new positions on the proximal floodplain area (Nichols & Fisher, 2007). The bounding surfaces that dip towards the palaeoflow direction correspond to downstream accretion elements (Miall, 1977), which develop during repeated flood events and macroform aggradation (Magalhães *et al.* 2014). The general fining-upward trend could be related to either systematic migration of the channels or to decrease in the flow energy through diversion (Bridge, 2006).

Table 1. Summarizing table of facies and facies associations and their main characteristics, in relation to sedimentary structures, depositional environments and appearance in the Northern Sydney Basin

Facies	Description	Sedimentary structures	Facies interpretation	Appearance
F1: Clast- to matrix-supported conglomerate.	Thick, amalgamated beds with an often tabular geometry or erosional base. Poorly to well-sorted and sub- to well-rounded clasts ranging from 0.2 to 10 cm in length and a sedimentary/igneous source	Structureless, in places reverse to normal grading.	Bedload transport during high flow regime. Clast-supported nature indicates action by braided streams (Nemec & Steel, 1984). Rounded pebbles suggest significant transport distance (Nichols, 1999) and clast imbrication points at tractional deposition (Whiting et al. 1988).	FA1, FA2
F2: Cross-stratified conglomerate.	Granular conglomerate that holds common planar and less common cross-stratification dipping between 30° and 40°. Clasts are rounded ranging from 0.2 to 5 cm in length and indicate a sedimentary/igneous source.	Both planar and trough cross-stratification, often mud drapes.	High-energy, channelized deposits formed by migration and deposition of gravelly barforms in a tidally influenced channel during the lower flow regime (Allen, 1983; Plink-Björklund, 2005).	FA1, FA2
F3: Structureless sandstone.	Amalgamated sandstone beds with poor sorting and fine to coarse grain size. Beds are often tabular with either sharp or erosional boundaries.	Unstratified.	Rapid deposition of high-density flows indicating high sedimentation rates that prevent efficient sorting (Lowe, 1988; Magalhães et al. 2015).	FA1, FA2, FA3,
F4: Trough cross-stratified sandstone.	Trough cross-bedded sandstone with moderate to well-sorted, fine to very coarse grains. F4 contains both single sets and co-sets separated by bounding surfaces often highlighted by mud drapes or pebbles.	Trough cross-stratification, often mud drapes.	Migration of S-shaped 3D dunes in lower-flow-regime conditions. S-shape dunes flow at relatively high speeds, with 3D growth occurring from separation vortices in the lee side of the dune (Miall, 1996).	FA1, FA2, FA3,
F5: Planar cross-stratified sandstone.	Coarse-grained, occasionally pebbly sandstone with low-angle inclined beds with dips varying between 25° and 40°. Bedforms are presented as either tabular or lenticular bodies.	Tabular to wedge-shaped cross-stratified sandstone. In places mud drapes.	Migration of straight-crested dunes in a tidally influenced channel (Reineck & Wunderlich, 1968). Low-angle cross-stratified sandstone and pebbly sandstone are related to plane bed deposition during or close to the upper flow regime (Collinson et al. 2006; Miall, 2014).	FA1, FA2, FA3,
F6: Compound cross-stratified sandstone.	Medium- to thick-bedded, stacked sets of both trough and planar cross-stratified sandstone. F6 forms both tabular and lenticular units with co-sets being separated by first-order bounding surfaces and often pebbles.	Cross-stratification, reactivation surfaces, superimposed ripples. In places mud drapes.	Repetitive migration of smaller straight- and sinuous-crested dunes (Miall, 1988). Co-sets separated by first-order set boundaries represent repeated bedform migration over larger bedforms (Ashworth et al. 2011; Miall, 2014).	FA1, FA2
F7: Ripple cross-laminated sandstone.	Fine- to medium-grained sandstone with moderate to well sorting and including mud laminae or mud drapes. Ripples are typically asymmetric and bimodal, and beds typically display a lenticular shape and fine upwards.	Asymmetrically ripple cross-lamination. Common mud drapes.	Migration of complex ripples in a tidally influenced environment corresponding to relatively weak currents during the lower flow regime (Collinson et al. 2006). Asymmetrical and bimodal ripples indicate oscillatory periodic flow and flow reversal (Reineck & Wunderlich, 1968).	FA1, FA2, FA3
F8: Horizontally- to low-angle-laminated sandstone.	Fine- to coarse-grained sandstone with poor to moderate sorting. Beds are often tabular, forming horizontal or low-angled lamination, typically 15° or less.	Parallel lamination, in places superimposed ripples.	Plane bed deposition during or close to the upper flow regime that is too shallow to have been reworked into subcritical bedforms (Alexander & Fielding, 1997).	FA1, FA2, FA3
F9: Contorted sandstone.	Fine- to medium-grained sandstone with irregular, deformed beds. Typically exhibit sharp boundaries with underlying beds and are laterally discontinuous.	Folded and overturned cross-stratification.	Deposition through traction currents and deformation by vertical shear occurring during high-discharge events and/or by the action of water escape and bedform collapse (Moretti et al. 2001).	FA2
F10: Hummocky/swaley cross-stratified sandstone.	Medium-grained sandstone with both “smile-like” hummocky cross-stratification and “frown-like” swaley cross-stratification. Beds form in sheet-like, tabular morphologies with either erosional or sharp boundaries.	Long smile- and frown-like structures in sandstone.	Infilling of sand infilling scours left as the result of oscillatory flows and unidirectional storm currents below the fair-weather wave base (Leckie & Walker, 1982; Myrow & Southard 1991).	FA3

(Continued)

Table 1. (Continued)

Facies	Description	Sedimentary structures	Facies interpretation	Appearance
F11: Heterolithic deposits.	Fine- to medium-grained sandstone with interbedded mudstone exhibiting flaser, wavy and lenticular bedding. Beds are tabular to lenticular with sharp or gradational bases.	Horizontal, wavy, lenticular and flaser lamination. In places mud drapes.	Bedload transport during tidal flow and suspension settlement during slack-water periods, leading to observed cyclic mud and sand beds (Martin, 2000).	FA2
F12: Structureless mudstone.	Light to dark grey mudstone that forms both lenticular and tabular beds with both gradational and sharp boundaries.	In places, very weak parallel lamination.	Deposition of suspended sediments during low-energy periods (Bridge, 2006).	FA1, FA2, FA3
F13: Parallel-laminated mudstone.	Light to dark grey mudstone that forms both lenticular and tabular beds with thinner, darker bands between lighter-coloured mudstone.	Thin horizontal lamination, in places repetitions of mudstone and siltstone.	Deposition through low energy suspension, which is influenced by weak currents that rework the sediments into laminated units (Pontén & Plink-Björklund, 2007).	FA1, FA2, FA3
F14: Coal.	Black, shiny appearance with irregular geometries that often split with typically sharp and occasional erosional boundaries.	Local mudstone and tuffaceous intercalations.	Coal deposition occurs due to the preservation of organic matter and equilibrium between peat production and accommodation space creation (Martin <i>et al.</i> 2013).	FA2
F15: Faintly laminated and massive tuff.	Fine-grained volcanic ash with occasional parallel laminations and antidunes. Beds are laterally continuous and traceable for several kilometres.	Parallel lamination, in places cross-lamination.	Reworking, transport and deposition of volcanic material by water.	FA2

4.a.2. Sub-FA1b: mid-channel bars

Description:

Sub-FA1b consists of conglomerate and fine- to very coarse-grained (and pebbly) sandstone that form thick (1–2.5 m) and laterally extensive (up to 6 m) sedimentary bodies (Fig. 6a). The main lithofacies include cross-stratified conglomerate (F2), trough (F3) and planar cross-stratified sandstone (F4) (Fig. 6b). These foresets are 0.5–1 m thick, exhibit lateral and vertical stacking, and form thicker (up to 2.5 m) co-sets. The sets are separated by first-order set boundaries, and the co-sets are bounded by second-order surfaces. First- and second-order bounding surfaces are characterized by sub-horizontal, sharp and often erosional contacts with the underlying units (Fig. 6c). The cross-beds are generally steeper-inclined (up to 25°), compared to the associated set and co-set bounding surfaces (up to 15° and 10°, respectively). Occasionally, ripple-cross-laminated (F7) and, rarely, parallel-bedded sandstones (F8) are observed and are restricted to the uppermost parts of the sub-FA1b. Both inclined and sheet-like heterolithic beds occur in some of the sub-FA1b deposits (Fig. 6d, e, f). The heterolithic beds form 0.5–1 m thick sets that exhibit repetitions of flaser, wavy and lenticular bedding. Commonly, individual cross-beds in the sets are truncated by first-order reactivation surfaces, and in some cases the toesets of individual cross-strata become indistinct, evolving into thin (3–8 cm) pebbly sandstone layers. Occasionally, the upper bounding surface displays a characteristic convex-down shape (Fig. 6d, g). In spite of the variety in the angle of dip, the surfaces associated with foresets, sets and co-sets vary in their respective dip inclinations, and exhibit similar mean azimuths to the SW or SE, in agreement with the main palaeodispersal direction.

Interpretation:

Sub-FA1b is interpreted as the result of migration of barforms in a downstream direction. This sub-facies is interpreted as mid-channel bar deposits that have been deposited in a fluvial environment. The regular changes between flaser, wavy and lenticular bedding are interpreted as rhythmites reflecting the impact of tides in some of the sub-FA1b deposits. The presence of inclined heterolithic bedding in some of the deposits of sub-FA1b suggests migration of barforms, such as mid-channel bars within a tidally influenced depositional setting, such as delta plain (Legler *et al.* 2013). The convex-down shape of the upper bounding surface further supports the mid-channel bar interpretation (Miall, 1977; Wakefield *et al.* 2015). The second-order surfaces are most likely related to the downstream migration of larger barforms, and the included planar and trough cross-bedded sandstone units reflect the migration of smaller straight- and sinuous-crested dunes (Miall, 1988). The erosional nature of these surfaces can be ascribed to either change in the palaeoflow direction and bar readjustment, or localized scour in front of advancing barforms (Miall, 2014). The co-sets that are separated by first-order set boundaries are associated with repeated bedform migration (train of dunes) over larger barforms (Ashworth *et al.* 2011; Miall, 2014). The reactivation surfaces suggest erosion that is related to short episodes of bedform adjustment, as a consequence of change in the rate and direction of the flow (Røe & Hermansen, 2006). Both inclined cross-beds and first- and second-order bounding surfaces display similar azimuths and demonstrate that both the smaller-scale dunes and the larger-scale bars migrated in the same direction. These features are in agreement with a downstream accretion element (Miall, 2014).

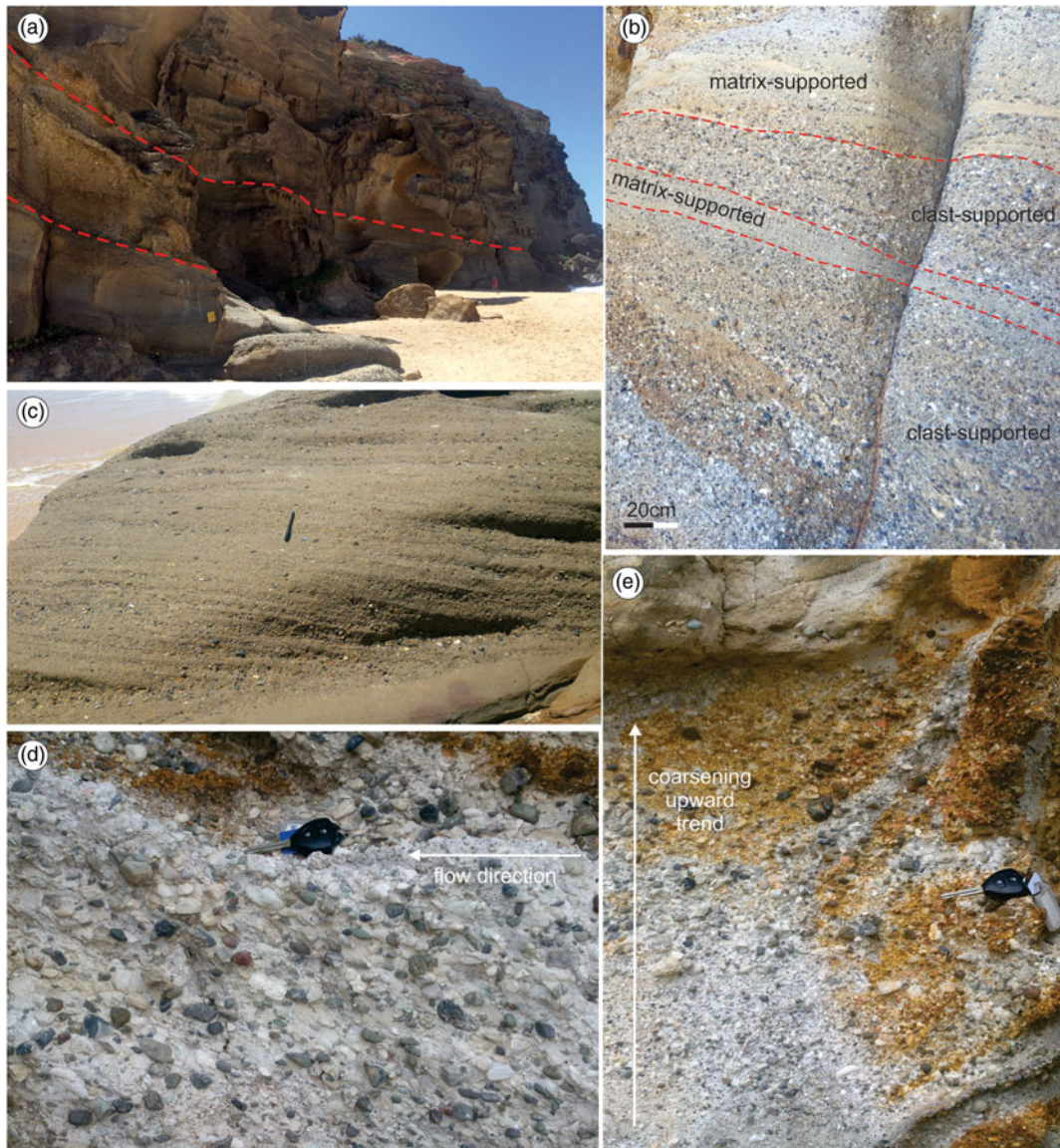


Fig. 4. (Colour online) Outcrop photographs illustrating diagnostic features of the fluvial sediments in the Northern Sydney Basin. (a) Repetitions of thick-bedded and coarse-grained sandstone with conglomerate. Note the bounding surfaces that dip towards the palaeoflow direction. (b) Repetitions of matrix- and clast-supported conglomerate. (c) Planar cross-stratified conglomerate. Note the abundant rounded pebble-grade extraclasts. (d) Clast-supported conglomerate with clast imbrication. The arrow points to the palaeoflow directions (to the left). (e) Reverse-grained conglomerate. Note the coarsening-upwards trend. Notebook for scale is 25 cm long. Key for scale is 8 cm long. Pen for scale is 15 cm long.

4.b. FA2: delta-plain deposits

Facies Association 2 (FA2) is *c.* 40 m thick. FA2 exhibits depositional elements that are present in a delta-plain depositional environment, such as distributary channel (sub-FA2a), ribbon channel (sub-FA2b), lateral bar (sub-FA2c), overbank (sub-FA2d), coal-prone floodplain (sub-FA2e) and crevasses splay deposits (sub-FA2f).

4.b.1. Sub-FA2a: delta-plain distributary channels

Description:

Sub-FA2a is sand-rich and primarily composed of thin- to very thick-bedded (0.2–1.5 m), fine- to very coarse-grained sandstone interbedded with thin- to medium-bedded (0.1–0.3 m) mudstone (Fig. 7a). Clast- to matrix-supported conglomerate (F1) and cross-stratified conglomerate (F2) occur in sub-FA2a, but are finer-grained,

thinner-bedded and less laterally continuous, compared to sub-FA1a. The sandstone of sub-FA2a is moderately to poorly sorted. Sandstone bodies appear as stacked sets that are mainly composed of thick beds of structureless (F3), trough cross-stratified (F4) and/or planar cross-stratified sandstone (F5). Often, structureless sandstone occupies the lower parts of the beds and is replaced upward by trough- or planar-cross-stratified sandstone (Fig. 7b). In places, cross-bedded sandstone is steeply dipping (20–30°) and may include and be overlain by mud drapes (Fig. 7c). Ripple cross-laminated sandstone (F7) and horizontally laminated sandstone (F8) are less common at the top of the thicker beds or may be the principal lithofacies in thinner beds (Fig. 7d). In addition, contorted sandstone (F9) and heterolithic deposits (F11) are present. Contorted sandstone displays folded and overturned cross-stratification. It comprises fine- to medium-grained sandstone with irregular, deformed beds (Fig. 7e). The heterolithic beds form mostly sand-dominated packages (flaser bedding),

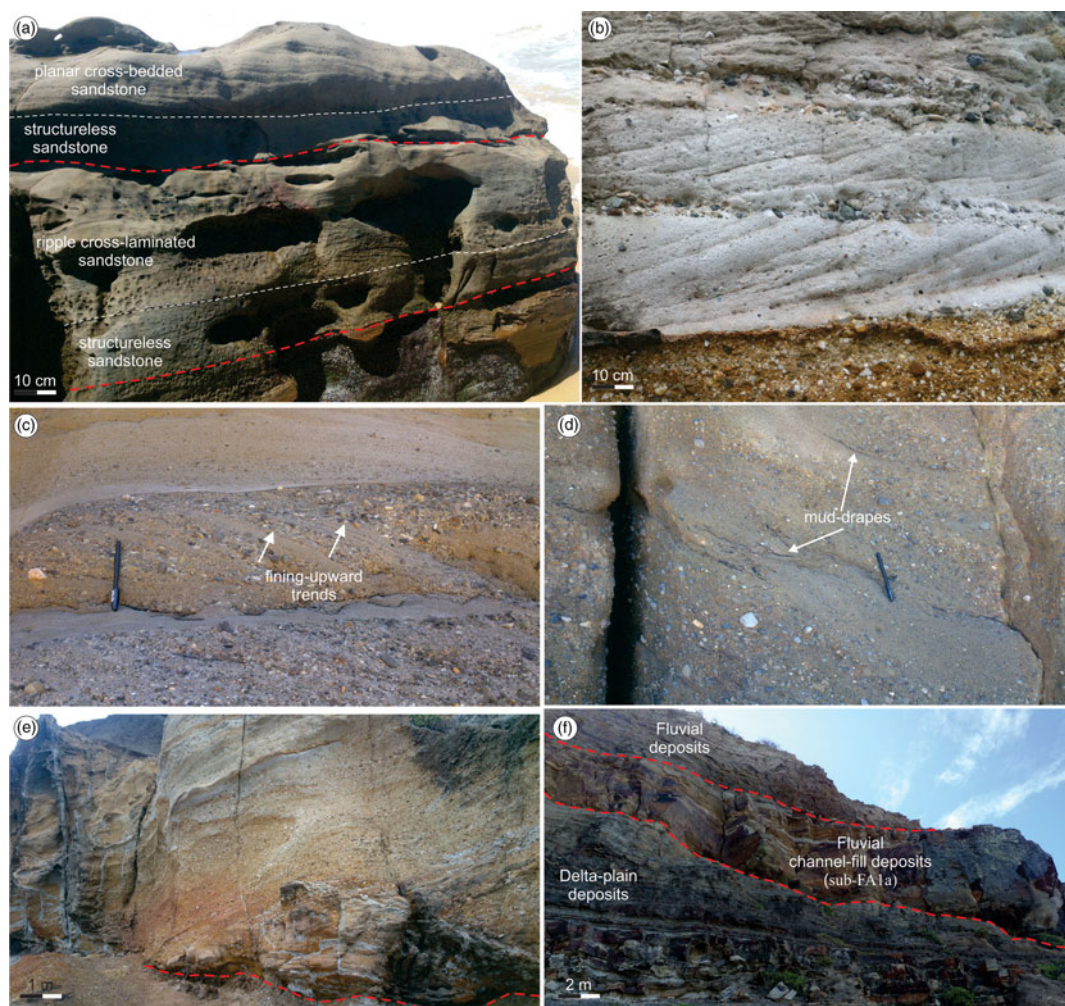


Fig. 5. (Colour online) Outcrop photographs illustrating diagnostic features of the fluvial sediments in the Northern Sydney Basin. (a) Structureless sandstone that overlays ripple cross-laminated and planar cross-bedded sandstone. (b) Co-sets of trough-cross-stratified sandstone. Note the bounding surfaces that separate the co-sets and are often highlighted by pebbles. (c) Cross-bedded sandstone with alternating foresets of sandstone and conglomerate within cross-beds. (d) Scattered mud drapes within the fluvial deposits. (e) Thick conglomeratic sediments that exhibit erosional contacts with the underlying sediments. (f) Fluvial channels that erode the underlying overbank and/or floodplain deposits and evolve laterally into overbank sediments. Pen for scale is 15 cm long.

whereas packages with equal sandstone–mudstone contents (wavy bedding) also occur (Fig. 7f). Internally, sandstone is structureless (F3) and/or ripple cross-laminated (F7), with these ripples having sometimes opposite dip directions.

Mudstone is usually structureless (F12), but often parallel-laminated (F13). Sub-FA2a contains abundant coal chips, wood fragments and petrified logs/branches, as well as thin (2–7 cm thick) coal beds (F14). Sub-FA2a exhibits sharp and/or erosional contacts with the underlying deposits and develops an erosional relief of 0.2–0.5 m (Fig. 8a). Such a feature leads to a concave-up basal scour surface, with a low topographic relief. These erosional surfaces are frequently highlighted by mud clasts and coarser grain sizes (Fig. 8a). Individually, the bed contacts can be erosional, gradational or sharp, with the latter two being gradually more prevalent towards the top of the sub-FA2a. Common sedimentary structures that are observed in this sub-FA include: abundant mud drapes and double mud drapes, tidal bundles and oppositely dipping current ripples (Fig. 8b, c, d). The bundles are bounded by mud drapes, and illustrate systematic thickness variations, from several millimetres to a few centimetres. These structures occur in most sandstone facies (less often in structureless sandstone) but are abundant in ripple cross-laminated sandstone and heterolithic deposits. Larger-scale

cross-stratified sandstone (0.3–1 m thick) bodies are also present within this sub-FA. Sub-FA2a consists of thick (3–8 m) packages of strata that are composed of stacked cycles with a characteristic fining-upward trend.

The basal parts of these cycles are composed of very thick-bedded sandstone (1–2 m) that evolves upwards into repetitions of thick- (0.5–1 m) and medium-bedded (0.1–0.2 m) sandstone with thin- to medium-bedded mudstone (0.05–20 cm). These sedimentary packages form thick bodies that can be laterally extensive for up to hundreds of metres (Figs 7a, 8e and Fig. 11a below). Sub-FA2a is associated with sub-FA2d (overlays, and also evolves laterally) and sub-FA2e (overlays). In places, sub-FA2a forms amalgamated sandbodies that are 8–15 m thick (Fig. 8e). Elsewhere, single sandstone beds erode in the underlying mudstone beds (Fig. 8f).

Interpretation:

Sub-FA2a is interpreted as tidally influenced channelized deposits in a delta-plain setting, with relatively shallow and narrow channels that cut into underlying fine-grained overbank and/or flood-plain deposits. This is supported by the basal erosion surfaces that document confined geometries, and the fining-upward trend that is ascribed to the upward waning of current energy (Bridge, 2006;

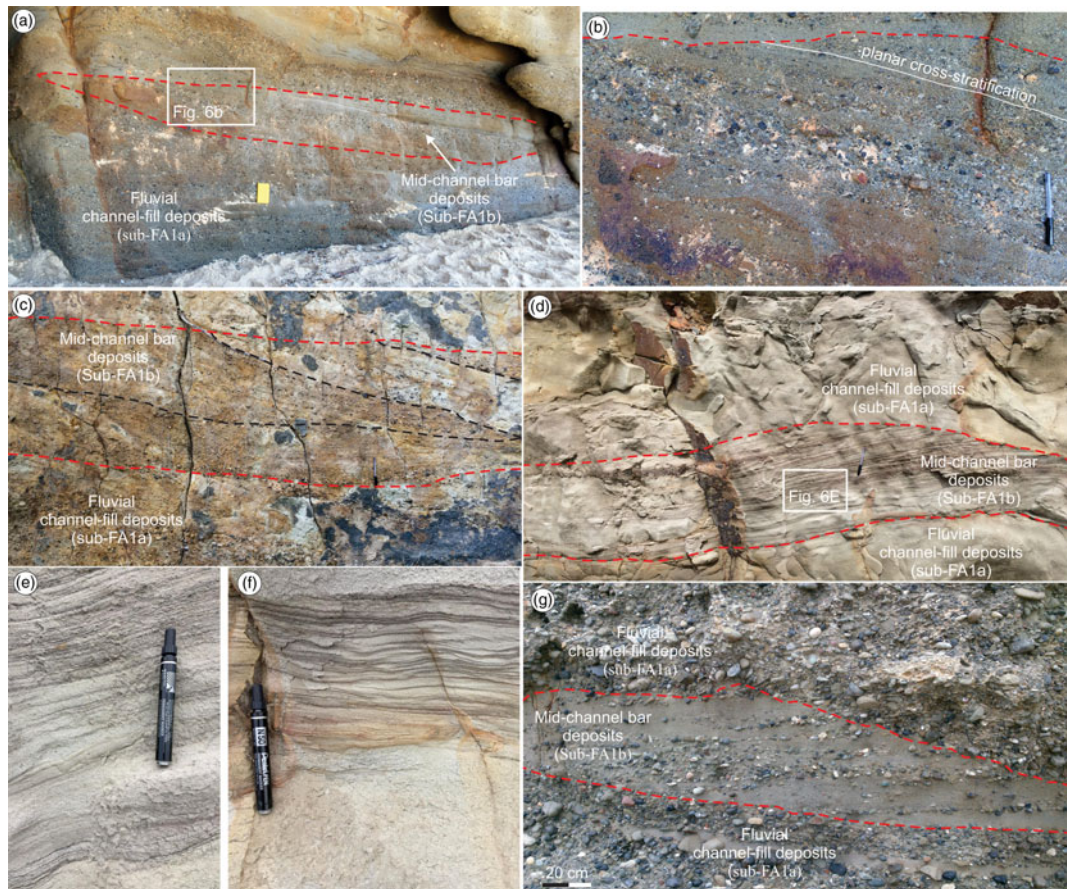


Fig. 6. (Colour online) Outcrop photographs illustrating diagnostic features of the mid-channel bar deposits in the Northern Sydney Basin. (a) Mid-channel bar deposits overlying channel sediments. Note the erosional contacts with the underlying units (b) Cross-bedded sandstone and conglomerate in the mid-channel bar deposits. (c) First- and second-order set boundaries that separate sets and co-sets. Note the sub-horizontal and/or erosional contacts with the underlying units. (d) Tidally influenced mid-channel bar deposits. Note the inclined heterolithic bedding that testifies the influence of tidal currents in these deposits. (e, f) Regular changes between flasher, wavy and lenticular bedding that are interpreted as rhythmites. (g) Characteristic convex-down shape of the upper bounding surface. Notebook for scale is 25 cm long. Pen for scale is 15 cm long.

Legler *et al.* 2013). The inclusion of coal and wood fragments, lack of marine bioturbation and presence of pebble-sized clasts, in conjunction with the prevalence of fluvial-related sedimentary structures (e.g. trough cross-bedding), suggest high-energy, fluvial style deposition (Visser, 1980; Nio & Yang, 1991). The contribution of tidal currents during the deposition of these sediments is documented by the abundance of single and double mud drapes, and by the presence of bipolar current ripples, tidal bundles and heterolithic beds (Cant & Walker, 1978; Mellere & Steel, 1996). Mud drapes reflect deposition during slack periods. The double mud drapes document deposition within the zone of tide dominance (Dalrymple & Choi, 2007). The bipolar current ripples testify to the action of reversing tidal currents (Reineck & Wunderlich, 1968). Tidal bundle thickness variations are interpreted to record neap–spring cyclicity. Heterolithic bedding indicates deposition by sporadic tidal flows, leading to observed cyclic mud and sand beds (Martin, 2000).

Sub-FA2a shares similar features with sub-FA1a and illustrates the lateral migration of energetic and channelized depositional settings over their associated overbanks and floodplains. The principal differences are associated with the much better preservation of overbank deposits and the abundance of tidally influenced sedimentary structures in sub-FA2a compared to sub-FA1a. The preservation of adjacent overbanks in sub-FA2a could be associated with the fluvial style, and suggests a still braided, but a less confined

nature of these deposits compared to sub-FA1a. Less frequent channel migration probably prevented the removal of fine-grained sediment and facilitated the formation of overbanks in sub-FA2a (Nichols & Fisher, 2007).

4.b.2. Sub-FA2b: ribbon channels

Description:

Sub-FA2b forms single, isolated lenticular-shaped sedimentary bodies that are 1–1.5 m thick and 6–12 m wide (low width/thickness ratio; Fig. 9a). These bodies are filled with sandstone that is fine- to medium-grained and moderately sorted. Some vertical and lateral amalgamation is present in this sub-FA, although individual concave-up geometries typically remain well defined (Fig. 9b). These deposits pinch out laterally over short distances and display a fining-upward trend (Fig. 9a). Sandstone within the sub-FA2b is structureless (F3), planar cross-stratified (F5) and/or horizontally laminated. Structureless sandstone occurs at the base of the sandstone beds, whereas planar cross-stratified and/or horizontally-laminated sandstone is common towards the top of the beds (Fig. 9c). In some places, mud drapes and heterolithic bedding (flaser bedding, F11) occur (Fig. 9d). Sub-FA2b overlays and evolves laterally into repetitions of sandstone and mudstone beds that belong to sub-FA2d. The basal contacts with these underlying finer-grained strata are sharp and erosional, defining a concave-up geometry. The incision in the sub-FA2b



Fig. 7. (Colour online) Outcrop photographs illustrating diagnostic features of the delta-plain, distributary channel deposits in the Northern Sydney Basin. (a) Delta-plain, distributary channel sediments that exhibit erosional contacts with the underlying sediments. (b) Structureless sandstone that evolves upwards into cross-bedded and horizontally laminated sandstone. (c) Mud drapes overlying cross-bedded sandstone. (d) Parallel-laminated sandstone. (e) Contorted sandstone displaying folded and overturned cross-stratification. (f) Heterolithic beds that form sand-dominated packages (flaser bedding). Pen for scale is 15 cm long.

may reach 1 m, where the erosional relief is also the total thickness of the channel at its axis. Sub-FA2b is also associated with sub-FA2e.

Interpretation:

Sub-FA2b is interpreted as ribbon channels (single-threaded channels) that form in sediment-starved environments, based on the concave-up geometry and the fining-upward trend. These channels reflect short-lived flows and form as a result of channel incision into their surrounding fine-grained facies (Friend *et al.* 1986). They suggest that the deposition of sand took place until they become water- or sediment-starved (Friend *et al.* 1986), and eventually pinch out into overbank (sub-FA2d) deposits. The fining-upward sandstone that extends laterally from the core of the body of sub-FA2b (wings) is related to flooding episodes and associated emplacement of sand further into overbanks (Mohrig *et al.* 2000).

4.b.3. Sub-FA2c: lateral bars

Description:

Sub-FA2c is commonly interbedded between coarse-grained deposits (sub-FA1a and mostly sub-FA2a) or overlays fine-grained sediments (sub-FA2d and/or sub-FA2e). It forms tabular to wedge-shaped, thick (1–3 m) sedimentary bodies that are laterally extensive (3–8 m). These deposits range from simple deposits, 0.5–1 m high, to complex bedforms up to 3 m high (Fig. 10a, b). The master bedding surfaces are planar and/or concave-up and are locally overlain by very thin bedded mudstone (a few mm thick).

The dip of the master bedding surfaces decreases towards the down-current parts of the sandstone bodies. Sub-FA2c is composed of medium- to very fine-grained sandstone and scarce pebbly sandstone. Component lithofacies include mainly planar cross-stratified sandstone (F5), but trough cross-stratified sandstone (F4) and, less often, structureless (F3) and/or horizontally laminated (F8) sandstone occur (Fig. 10c). The foresets are organized in a toplap, offlap and downlap relationship with the adjacent strata. The cross-beds commonly downlap abruptly onto the underlying deposits or onto the basal surface (Fig. 10c). Some of the cross-beds may fine upwards, commonly from pebbly- and coarse-grained sandstone at the base to medium- to very fine-grained sandstone at the top (Fig. 10c). Palaeocurrent data derived from cross-beds are oblique to the main palaeocurrent direction (refer to palaeocurrent analysis). Mud drapes and heterolithic bedding (flaser bedding) occur in some of these deposits. Basal surfaces with underlying strata are concave-up, sharp and commonly erosional. In some instances, the base of the sub-FA2c rests upon erosive surfaces that may extend beyond the lateral extents of this sub-FA.

Interpretation:

Sub-FA2c is interpreted as a lateral accretion element (lateral bar) indicating localized sinuosity in a channelized depositional environment. Supporting evidence derives from the dip of the cross-beds that is oblique to the main palaeoflow direction of the river channels, the tabular to wedge shape, the close association with channelized sediments (sub-FA2.1), and the dominance of planar and trough cross-stratification. These characteristics are indicative

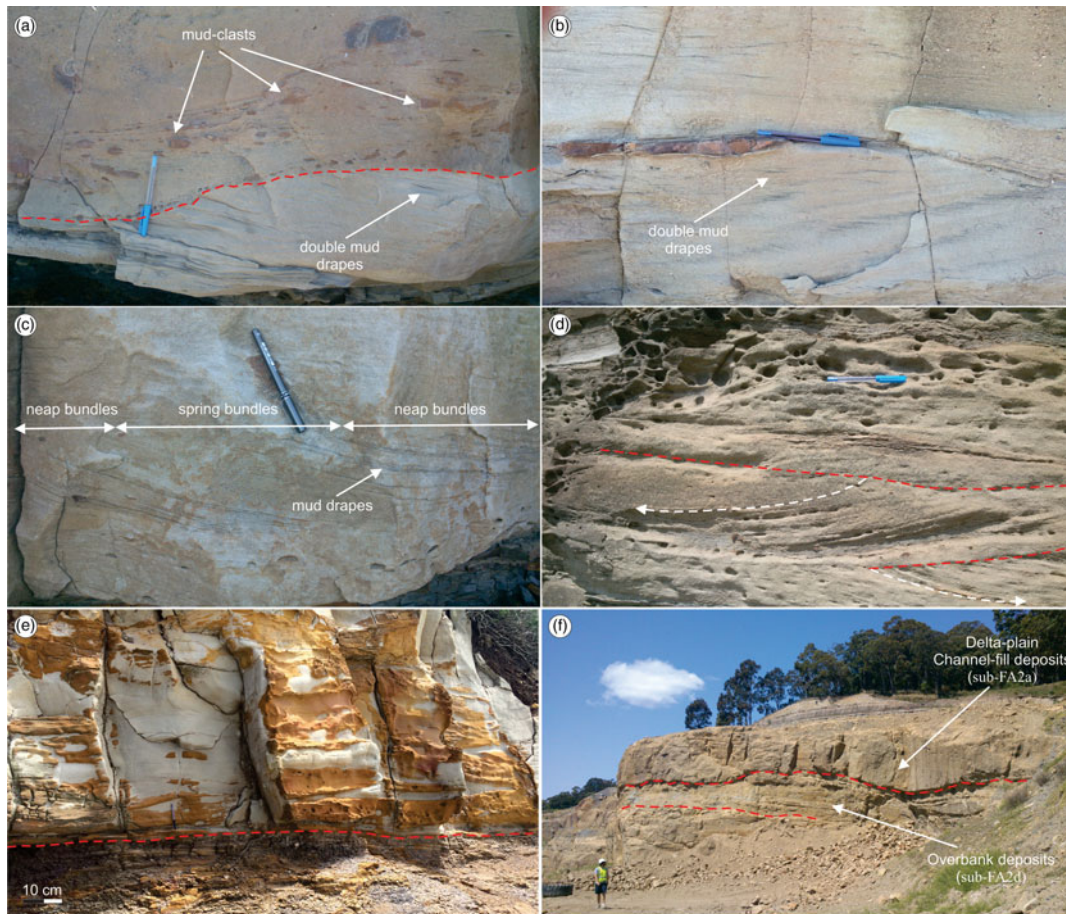


Fig. 8. (Colour online) Outcrop photographs illustrating diagnostic features of the delta-plain, distributary channel deposits in the Northern Sydney Basin. (a) Erosional surfaces that are highlighted by mud clasts. (b) Double mud drapes. (c) Tidal bundles reflecting deposition during neap and spring periods. (d) Bipolar current ripples. (e, f) Delta-plain, distributary channel deposits overlying overbank and/or floodplain deposits. Note the erosional contact with the underlying sediments. Person for scale is 180 cm tall. Pen for scale is 15 cm long.

of deposition in lateral bars that form along the margins of fluvial channels (Bridge, 2003). Where present, mud drapes and double mud drapes suggest the tidal influence in some of the sub-FA2c deposits (Pontén & Plink-Bjorklund, 2007). The master bounding surfaces that dip obliquely to the main palaeoflow direction are interpreted as lateral accretion surfaces and are consistent with the lateral bar interpretation of these deposits. The absence of erosion or reorganization, related to periods of low discharge, indicates that lateral accretion may have occurred coevally with downstream accretion. Similar features have been also described in other studies (Santos *et al.* 2014; Wakefield *et al.* 2015; Mellere *et al.* 2016).

4.b.4. Sub-FA2d: overbank deposits

Description:

Sub-FA2d is composed of thin- to medium-bedded (0.1–0.3 m) sandstone and mudstone, commonly associated with sub-FA1a, sub-FA2a and sub-FA2b. They are often interbedded between the underlying sub-FA2a and sub-FA2b and the overlying sub-FA2e (Fig. 11a). This sub-FA forms thick sedimentary successions (5–7 m). The sandstone is structureless (F3), ripple-cross-laminated (F7) and/or heterolithic-bedded (F11). Internally, the heterolithic beds comprise thin- to medium-bedded (2–25 cm thick) sand- to mud-dominated couplets. The sandy (flaser) parts contain current ripple cross-lamination (F3). The muddy parts are structureless

or parallel-laminated and may include very thin- to thin-bedded (1–10 cm) sandstone forming lenticular to wavy bedding (Fig. 11b). Rarely, an upward transition from flaser through wavy to lenticular bedding exists within the medium-bedded sandstone of the sub-FA2d (Fig. 11c). Mudstone beds are structureless (F12) and/or parallel-laminated (F13). The tops of the sandstone beds are often flat, but they often exhibit lenticular geometry (Fig. 11c). The bases of the sandstone beds are mostly flat, but in some cases record localized erosion. Sub-FA2d can be laterally extensive for up to several hundred metres. Sub-FA2d is common within the lower stratigraphic levels (in the deltaic section of the studied succession). Up-sequence (in the fluvial section of the succession), it contains more sand, becomes less common and is typically thinner.

Interpretation:

Sub-FA2d is interpreted as overbank deposits that form on top of inactive channels and adjacent to active channels in the delta plain. The thicker, fine-grained sandstone beds suggest that the energy of the depositional environment was low and located adjacent to the active channels (Nichols, 1999). The presence of fine-grained heterolithic bedding indicates tidal modulation during the deposition of some of the sediments (Reineck & Wunderlich, 1968). Parallel-laminated mudstone indicates that sub-FA2e was influenced by weak currents that reworked the sediments into laminated units (Pontén & Plink-Bjorklund, 2007). The lenticular geometry of

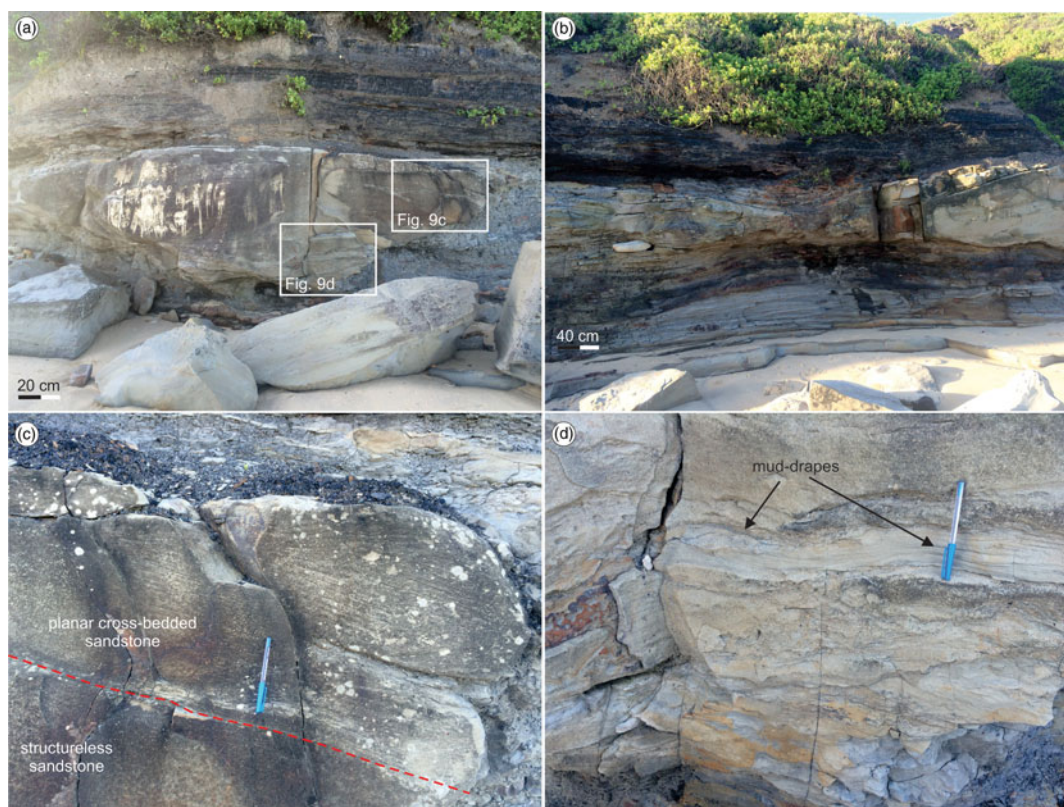


Fig. 9. (Colour online) Outcrop photographs illustrating diagnostic features of the ribbon channel deposits in the Northern Sydney Basin. (a) Lenticular-shaped sedimentary bodies with low width/thickness ratio. (b) Lateral amalgamation of ribbon channel deposits. (c) Planar cross-bedded sandstone occupying the upper parts of the deposits and underlain by structureless sandstone. (d) Mud drapes and heterolithic bedding observed at the base of the ribbon channels. Pen for scale is 15 cm long.

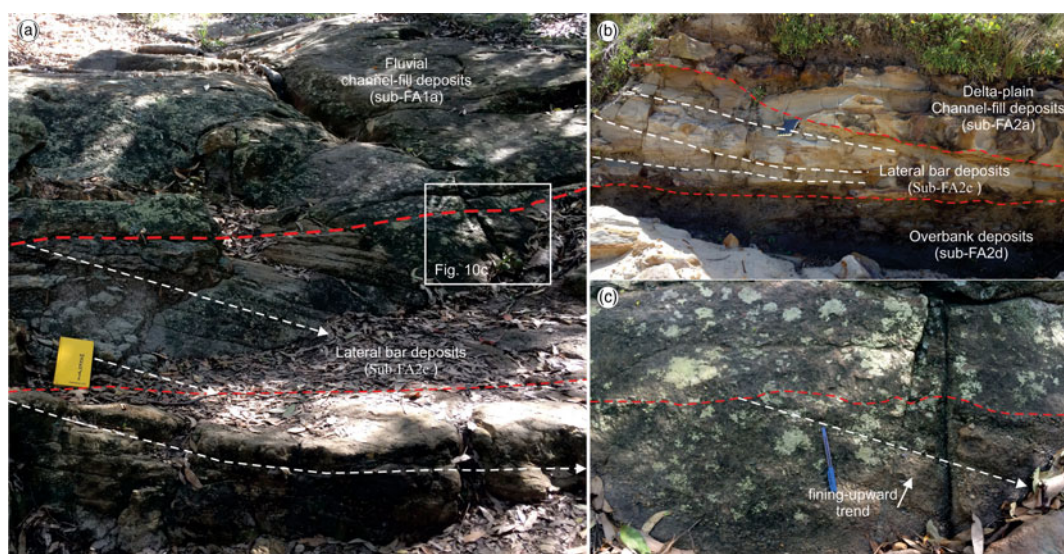


Fig. 10. (Colour online) Outcrop photographs illustrating diagnostic features of the lateral bar deposits in the Northern Sydney Basin. (a, b) Tabular to wedge-shaped, thick sedimentary bodies. Note the planar and/or concave-up master bedding surfaces. The dip of these surfaces decreases towards the downcurrent parts of the sandstone bodies. (c) Cross-beds that downlap abruptly on the underlying deposits. Note the fining-upwards trend in some of the cross-beds. Notebook for scale is 25 cm long. Pen for scale is 15 cm long.

the beds could be associated to sea floor instability, in agreement with overbank settings (Pontén & Plink-Bjorklund, 2007). The up-sequence decrease in abundance, thickness and grain size of the sub-FA2d indicates an increase in the erosion of the associated floodplain deposits (Nichols & Fisher, 2007). The association of

sub-FA2d with channelized deposits (sub-FA1a, sub-FA2a and sub-FA2b) suggests that this increased erosion was most likely associated with enhanced channel migration.

An alternative interpretation could be that this sub-FA corresponds to tidal flat deposits. However, the lack of regular variations

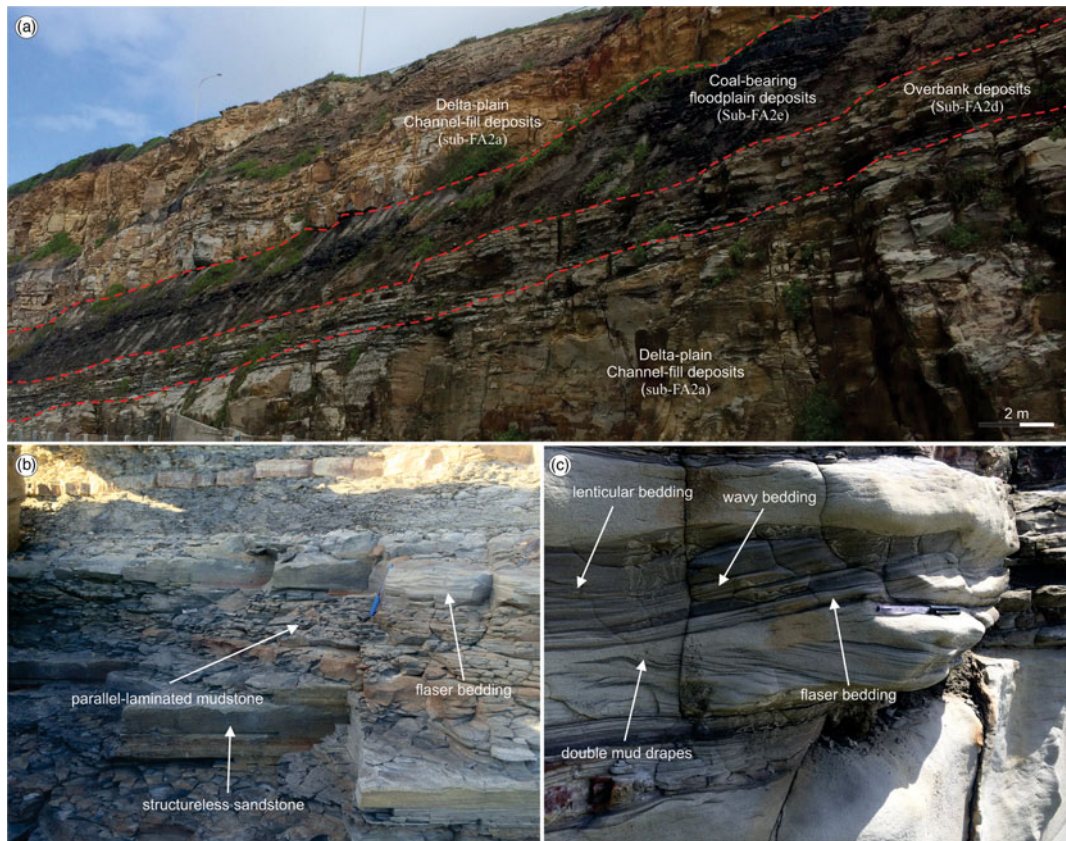


Fig. 11. (Colour online) Outcrop photographs illustrating diagnostic features of the overbank deposits in the Northern Sydney Basin. (a) Overbank facies interbedded between the underlying channelized and the overlying coal-bearing floodplain deposits. (b) Repetitions of structureless and heterolithic-bedded sandstone with mudstone. (c) Heterolithic bedding in the overbank deposits. Note the upwards transition from flaser to lenticular bedding. Pen for scale is 15 cm.

between flaser, wavy and lenticular bedding in an upward-fining fashion, a diagnostic feature of tidal flats (Dalrymple, 2010; Daidu, 2013), makes the overbank setting the most plausible interpretation for the sub-FA2d.

4.b.5. Sub-FA2e: coal-prone floodplain deposits

Description:

Sub-FA2e occurs on a range of scales from mm-sized ribbons to metre-thick (up to 8 m thick) beds (Fig. 12a). Coal appears as dull black to shiny black in colour and forms tabular beds that thin, split and pinch out laterally, interfingering with volcanoclastic sediments (Fig. 12b). Coal beds can be traced for hundreds of metres at the same stratigraphic levels and are characterized by a sharp boundary with the underlying heterolithic-bedded sandstone, structureless (F12) and/or parallel-laminated mudstone (F13) that belong to sub-FA2d (Fig. 12c). Often, coal deposits are overlain by sand-dominated beds of sub-FA2a.

Interpretation:

The formation of peat mires is associated with climatic conditions and availability of organic matter. Their formation requires humid, swampy conditions in areas where rainfall exceeds evaporation and organic growth is rapid (Guion *et al.* 1995). The great thickness of the coal deposits in the study area indicates prolonged periods of peat accumulation. In deltaic settings, coal beds can form under continuously rising mire water table (base level) relative to the sediment surface that generated the accommodation required for peat accumulation (Davies *et al.* 2006). A similar environment is

indicated for these deposits. Their association with delta-plain channelized deposits (sub-FA2a) reflects the lateral migration of the distributary channels that rest on the former, coal-bearing floodplain area.

4.b.6. Sub-FA2f: crevasse splays

Description:

Sub-FA2f is composed of thin- to thick-bedded (0.2–1 m), fine- to medium-grained sandstone that is mostly enclosed within mudstone (Fig. 13a). The surrounding mudstone is structureless (F12) or parallel-laminated (F13) and belongs to the sub-FA2d. The surrounding sediments may also include very thin- to thin-bedded (0.1–0.2 m) sandstone. The sandstone in the sub-FA2f is structureless (F3), horizontally laminated (F8) and/or ripple cross-laminated (F7) and displays a fining-upward trend (Fig. 13b). Mud drapes may be present in the cross-beds of some of the sandstone beds (Fig. 13c). The sandstone beds are 4–6 m wide and exhibit tabular to lenticular geometry. The beds have a maximum thickness of 11 m, and gradually decrease laterally before merging into the surrounding mudstone (Fig. 13a). The contacts with the underlying fine-grained sediments are sharp and/or erosional and incise a few centimetres down (1–15 cm). The upper bed contacts are often gradational and/or sharp.

Interpretation:

Sub-FA2f is interpreted as crevasse splay deposits that have been deposited in a deltaic depositional environment. Supporting evidence derives from the lenticular geometry of this sub-FA, the



Fig. 12. (Colour online) Outcrop photographs illustrating diagnostic features of the coal-bearing floodplain deposits in the Northern Sydney Basin. (a) Tabular-shaped, thick coal bed in the studied region. (b) Coal beds that thin, split and pinch out laterally, interfingering with volcanoclastic sediments. (c) Coal bed that exhibits sharp boundary with the underlying heterolithic-bedded sandstone and structureless mudstone that belong to overbank deposits. Pen for scale is 15 cm.



Fig. 13. (Colour online) Outcrop photographs illustrating diagnostic features of the crevasse splay deposits in the Northern Sydney Basin. (a) Thin- to thick-bedded sandstone that pinches out into the surrounding fine-grained overbank deposits. (b) Mud drapes in the cross-beds of some of the sandstone beds. (c) Ripple cross-laminated sandstone. Bag for scale is 45 cm long. Pen for scale is 15 cm.

association with overbank sediments (sub-FA2d) and the fining-upward trend. The thick (up to 1 m) sandstone beds that are enclosed between mud-rich sediments point to sporadic input of coarser material into a region of low energy. This sub-FA represents deposits that formed by breaching of overbank deposits by active channels and associated deposition in the floodplain/overbank areas (O'Brien & Wells, 1986). The sharp bases with the

underlying sediments and the fining-upward trend are associated with initial rapid flow that follows the break of the overbanks, which in turn is followed by subsequent waning. This waning reflects the decrease in the water and sediment availability through time (Nichols, 1999). Fast sediment input is interpreted from erosional basal contacts, capable of scouring and eroding the underlying mudstone, whereas the overlying gradational base indicates

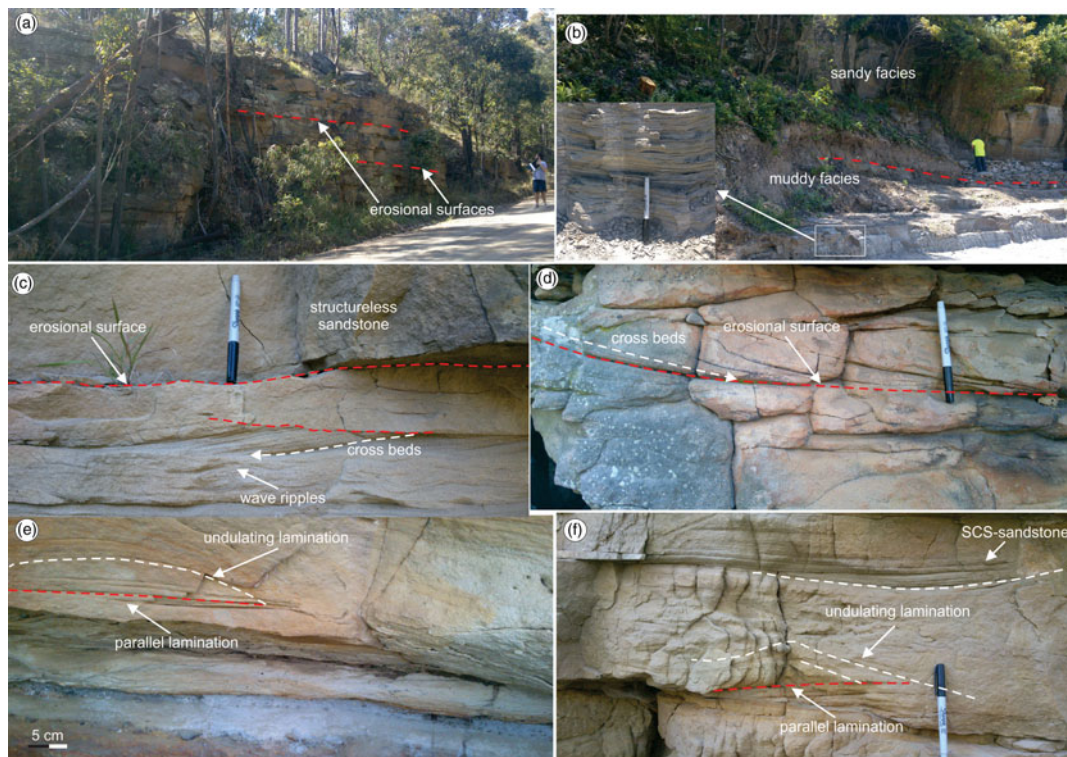


Fig. 14. (Colour online) Outcrop photographs illustrating diagnostic features of the delta-front deposits in the Northern Sydney Basin. (a) Thick amalgamated sandstone units. Note that the beds are separated by erosional surfaces. (b) Thickening- and coarsening-upwards trend in the studied deposits. (c) Cross-laminated sandstone that is overlain by structureless sandstone. Note the wave ripples below the cross-laminated sandstone. (d) Cross-bedded sandstone. (e) HCS-sandstone. Note the basal planar to low-angle laminated unit that is overlain by undulose lamination. (f) SCS-sandstone exhibiting low-angle lamination that infills basal scour surfaces. Pen for scale is 15 cm. Person for scale is 180 cm tall.

the steady reduction in sediment input and energy over time (Ethridge *et al.* 1999).

4.c. FA3: delta-front deposits

Facies Association 3 (FA3) is *c.* 251 m thick. FA3 exhibits features that are characteristic of a delta-front depositional setting including thick, amalgamated and medium- to well-sorted sandstone bodies that hold evidence of wave and storm influence. FA3 does not outcrop throughout the study area but does outcrop inland at outcrop 13 (Fig. 2).

4.c.1. Description

FA3 is sand-rich and forms a sedimentary succession that is composed of fine- to medium-grained, thin- to thick-bedded sandstone (0.1–1.21 m, Fig. 14a). Rarely, isolated pebbles or very thin pebbly layers (a few mm thick) have been observed. This FA exhibits a coarsening- and thickening-upward trend, and thus, mudstone is not abundant and is mainly restricted to the lower parts of the succession (Fig. 14b). Thin mudstone layers, up to 2 cm thick, may be present between sandstone beds. FA3 displays a variety of sedimentary structures (Fig. 14c, d, e, f). The sandstone beds can be structureless (F3), trough cross-stratified (F4), planar cross-stratified (F5), ripple cross-laminated (F7), horizontally laminated (F8) or hummocky/swaley cross-stratified (HCS and SCS respectively, F10). Oscillatory ripple cross-lamination is sometimes present and may occur at the tops of hummocky cross-stratified beds. Mudstone drapes are very rare.

Sandstone beds are commonly amalgamated, and form sets that are up to 41 m thick. Upper bed surfaces may be flat or undulose, and

locally are sharply overlain by thin-bedded mudstone. Internally, sandstone beds are separated by erosional surfaces (Fig. 14c). HCS and SCS, along with traction structures (e.g. planar and trough cross-bedding), are the dominant sedimentary structures in the FA3 deposits (Fig. 14d, e, f). HCS- and SCS-sandstone develops medium- to large-scale cross-stratification, in which the undulating and gently dipping laminae comprise large-amplitude (tens of cm) and low-relief (a few cm) hummocks and troughs (Fig. 14e, f). HCS-sandstone consists of a basal planar to low-angle laminated unit (1–5 cm thick) and is overlain by undulose lamination (Fig. 14e). SCS-sandstone exhibits low-angle lamination that often infills basal scour surfaces (Fig. 14f). Bioturbation is generally scarce. Rare vertical specimens of *Ophiomorpha* comprise the only ichnotaxon observed.

4.c.2. Interpretation

This facies association is interpreted here as delta-front deposits. The main lines of evidence come from the presence of HCS and SCS, as well as the stratigraphic position of these deposits that are sitting below delta-plain (FA2) deposits. The HCS and SCS have long been regarded as storm-related sedimentary structures (Leckie & Walker, 1982), whereas the isolated wave ripples may record wave reworking during the waning stage of a storm, or fair-weather reworking (De Raaf *et al.* 1977). Massive to planar-laminated sandstone below HCS-sandstone records initial erosion and subsequent fallout from suspension. The low-angle lamination in SCS-sandstone that mantles scours represents relatively low aggradation rates and the preferential preservation of troughs (swales) rather than mounds (Dumas & Arnott, 2006). The structureless sandstone beds may indicate periods of high sedimentation rates. The thick, sandstone

Table 2. Summary of palaeocurrent measurements, in relation to depositional environments in the Northern Sydney Basin

Depositional environment of measurements	Mean palaeocurrent direction	Corresponding rose diagram	Number of measurements
Delta plain	165°	15 (A)	19
Delta plain	201°	15 (B)	23
Delta plain	171°	15 (C)	24
Delta plain	169°	15 (D)	22
Delta plain	184°	15 (E)	17
Delta plain	190°	15 (F)	27
	174°	15 (G)	16
	169°	15 (H)	21
	196°	16 (A)	27
	203°	16 (B)	38
	182°	16 (C)	18
	199°	16 (D)	17

beds of FA3 are interpreted as the results of combined effect of continuous supply of relatively coarse material, along with deposition within a turbulent environment (Myrow & Southard, 1991).

The cross-bedded sandstone is interpreted as being deposited by dunes. Similar cross-stratification, with high dip angle and large set thickness, can be produced by waves in coarse-grained sandstone (Leckie, 1988; Cummings *et al.* 2009). The fine grain size of this FA indicates that these cross-stratified sandstone beds represent unidirectional traction structures, further suggesting a high-energy delta-front environment of deposition for the FA3. The general absence of mudstone in the succession is also compatible with a high-energy delta-front environment (Pemberton *et al.* 2002). The overall coarsening-upward trend could be indicative of mouth bar progradation and corresponds to the unconfined deposits accumulated at the mouths of the distributary channels. Structureless sandstone most likely accumulated during high discharge periods and is indicative of river floods, documenting the influence of river currents during deposition (Rossi & Steel, 2016). The very low (nearly absent) degree of bioturbation is probably associated with hostile environmental conditions that are ascribed to increased fluvial input, and is in agreement with deposition in a high-energy setting (MacEachern & Bann, 2008). It suggests environmentally stressed conditions (e.g. increased turbidity or lowered salinity), which could reflect proximity to delta distributary mouths (MacEachern & Bann, 2008).

5. Palaeocurrent analysis

Palaeocurrent analysis was conducted within both the deltaic and the fluvial portion of the succession. Paleoflow data were collected from several outcrops. In particular, 21 measurements were taken from one outcrop from the delta-front deposits, 148 measurements were collected from seven outcrops from the delta-plain sediments and 100 measurements were collected from four outcrops from the fluvial deposits (Table 2).

The data exhibit a SE- to SW-directed transport direction indicating a NW- to NE-located sediment source. These results agree with previous studies that also indicate a predominantly north to south operating routing system with a slight NE to SW shift

(G Fay, unpub. Honours thesis, Univ. Newcastle, Australia, 1980; PR Warbrooke, unpub. Ph.D. thesis, Univ. Newcastle, Australia, 1981). However, the studied succession records a complex palaeocurrent pattern, with major routing systems flowing both axially and transverse to the principal uplift structures in the New England Orogen, such as the Peel–Manning Fault System (Collins, 1991). In particular, the data from the delta-front and delta-plain deposits indicate a S, SE (axial) transport pathway (Fig. 15), whereas the overlying fluvial sediments exhibit a mostly SW (transverse) palaeoflow pattern (Fig. 16).

6. Stratigraphy

The studied succession (*c.* 901 m thick) was examined by logging and correlating 13 laterally extensive (hundreds of metres) outcrops, with all but one (outcrop 13) being situated along the 25 km of coastline (Fig. 2). Delta-front deposits (FA3, 251 m thick) are restricted to one outcrop (outcrop 13). Delta-plain deposits (FA2, 40 m thick) correspond to the bulk volume of the studied succession and are exposed in almost all studied outcrops (except outcrop 12). The fluvial sediments (FA1, 25 m thick) correspond to a considerable volume of the studied succession and are exposed at several outcrops (Figs 17–19). The outcrops illustrate the vertical and lateral facies transitions evident in different parts of the delta system. From northeast to southwest, the region exhibits a general trend from delta-front deposits (FA3), through delta-plain sediments deposited below the tidal limit (FA2), to fluvial channels above or close to the inferred tidal limit (FA1). Similarly, the overall vertical transition through the succession (Figs 17–19) is from delta-front sediments (FA3) into delta-plain deposits (FA2), overlain by fluvial and mostly channelized deposits (sub-FA1a). The boundary between the delta-front and delta-plain deposits was not observed, but the boundary between the delta-plain and fluvial can be traced in several outcrops across the entire study region and is represented by an extensive erosion surface (Figs 18, 19). This fluvio-deltaic system was impacted by volcanic activity, as evidenced by the occurrence of tuff units (Figs 17, 18). The principal volcanic activity is well constrained at the boundary between the delta-plain and fluvial sediments.

In sequence-stratigraphic terms, the progradation and aggradation recorded by the studied deltaic system indicate deposition during a normal regression of the shoreline (Catuneanu, 2017). The abrupt increase in grain size from the deltaic system to the overlying fluvial system also indicates an increase in topographic gradients and energy levels across the subaerial unconformity, which is typical of the contrast between highstand (lower energy, at the top of a depositional sequence) and lowstand (higher energy, at the base of a depositional sequence) conditions (Catuneanu, 2006). Therefore, the deltaic system is interpreted as the foreset (delta front) and the topset (delta plain) of a highstand systems tract, whereas the overlying fluvial system is interpreted as the topset of a lowstand systems tract. The depositional patterns recorded in this case study are similar to the trends documented in other sedimentary basins along the southern margin of Gondwana, during the Permian (Rubidge *et al.* 2000).

7. Discussion

7.a. Controls of depositional processes on sedimentation

Tidally influenced regressive, deltaic settings still need further research in order to improve our understanding of their development.

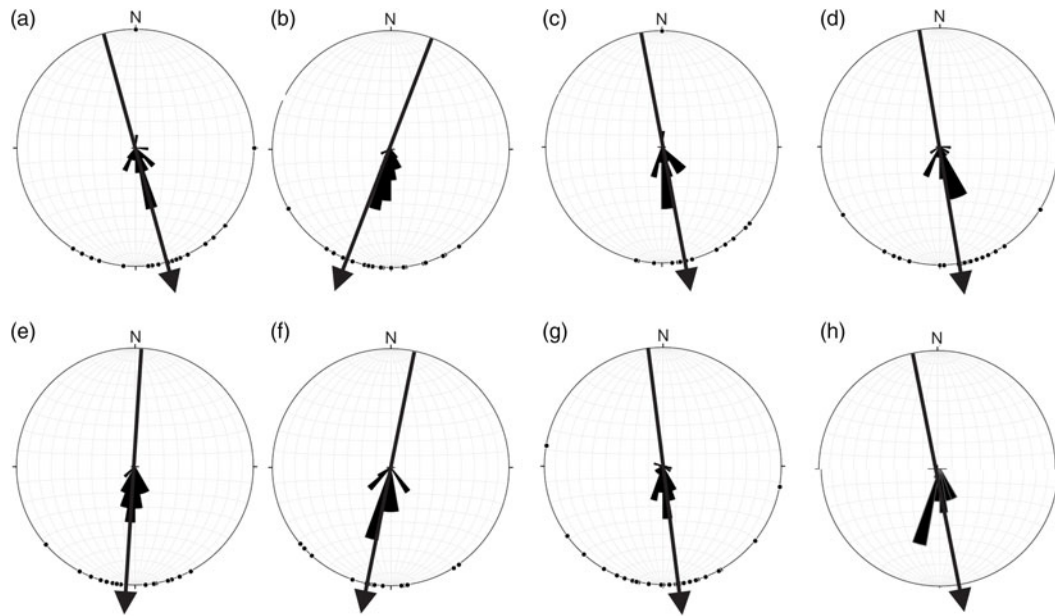


Fig. 15. Rose diagrams (a–h) illustrating the measured values and the mean palaeocurrent direction in the delta-plain deposits. Note the main S-SE palaeodispersal direction.

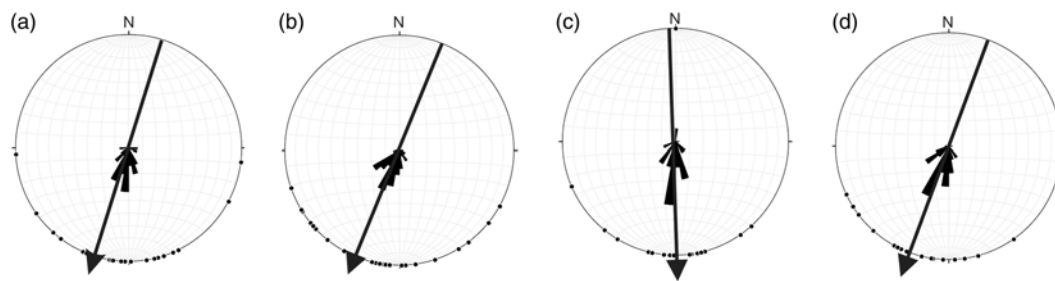


Fig. 16. Rose diagrams (a–d) illustrating the measured palaeoflow values and the mean direction in the fluvial deposits. Note the main S-SW palaeodispersal direction.

Outcrop-based sedimentologic and stratigraphic models are not abundant, but include the Cretaceous Sego Sandstone, Utah, USA (Willis & Gabel, 2003), the Jurassic Lajas Formation, Argentina (McIlroy *et al.* 2005; Rossi & Steel, 2016), the Devonian Amata and Gauja Formations, Latvia and Estonia (Pontén & Plink-Björklund, 2007; Tänavsuu-Milkeviciene & Plink-Björklund, 2009), and the Eocene lower Dir Abu Lifa Member, Western Desert, Egypt (Legler *et al.* 2013). In addition, similar settings have been described based on well datasets (Middle Jurassic Bryne Formation, Norwegian North Sea, Mellere *et al.* 2016).

The sedimentological study presented here indicates an upward shift of the depositional environments and sub-environments from delta-front to delta-plain and fluvial deposits. This trend, in conjunction with the palaeoflow directions, indicates progradation of the fluvio-deltaic system towards the SSE and SSW (Fig. 20). The sedimentary succession reflects the interplay of river, wave and tidal currents. The lowermost delta-front deposits were mainly controlled by wave and storm action, indicated by wave ripples and HCS, with no sedimentological evidence for tidal influence. The overlying delta-plain deposits reflect a change in the dominant processes that controlled deposition. These sediments were impacted by the interaction of river and tidal currents. Sedimentary structures that testify concurrent tidal action include: mud drapes, bidirectional current ripples, tidal bundles, flaser, wavy and lenticular bedding. These structures

are abundant in the delta-plain deposits (in both distributary channels and overbanks). River influence is recognized by the abundant wood debris and high degree of internal erosional surfaces. No significant wave influence has been recorded in the studied delta-plain deposits, suggesting weak wave interaction during sediment deposition.

The overlying fluvial deposits display a predominant river influence. This is documented by: (1) the high degree of amalgamation and internal erosional surfaces, (2) the coarse grain size (cobbles and pebbles), (3) the lack of bioturbation, and (4) the abundant plant debris. Sporadic mud drapes may be related to tidal modification of river currents. Nevertheless, the lack of organization in the drapes makes this scenario unlikely (Ichaso & Dalrymple, 2014; Rossi & Steel, 2016). Similar characteristics have been described in the Middle Devonian Gauja Formation in the Baltic Basin, Latvia and Estonia (Pontén & Plink-Björklund, 2007). In the Gauja Formation, tidal and fluvial processes control the sediment accumulation, but the wave influence is of secondary importance. Like the studied NSB succession, the Gauja Formation displays an upwards decrease in tidal influence, and an absence of sedimentary structures that would suggest wave action. These features have been associated with a gradual increase in the fluvial input and with the sufficiently strong tidal currents that were capable of suppressing the wave action (Pontén & Plink-Björklund, 2007).

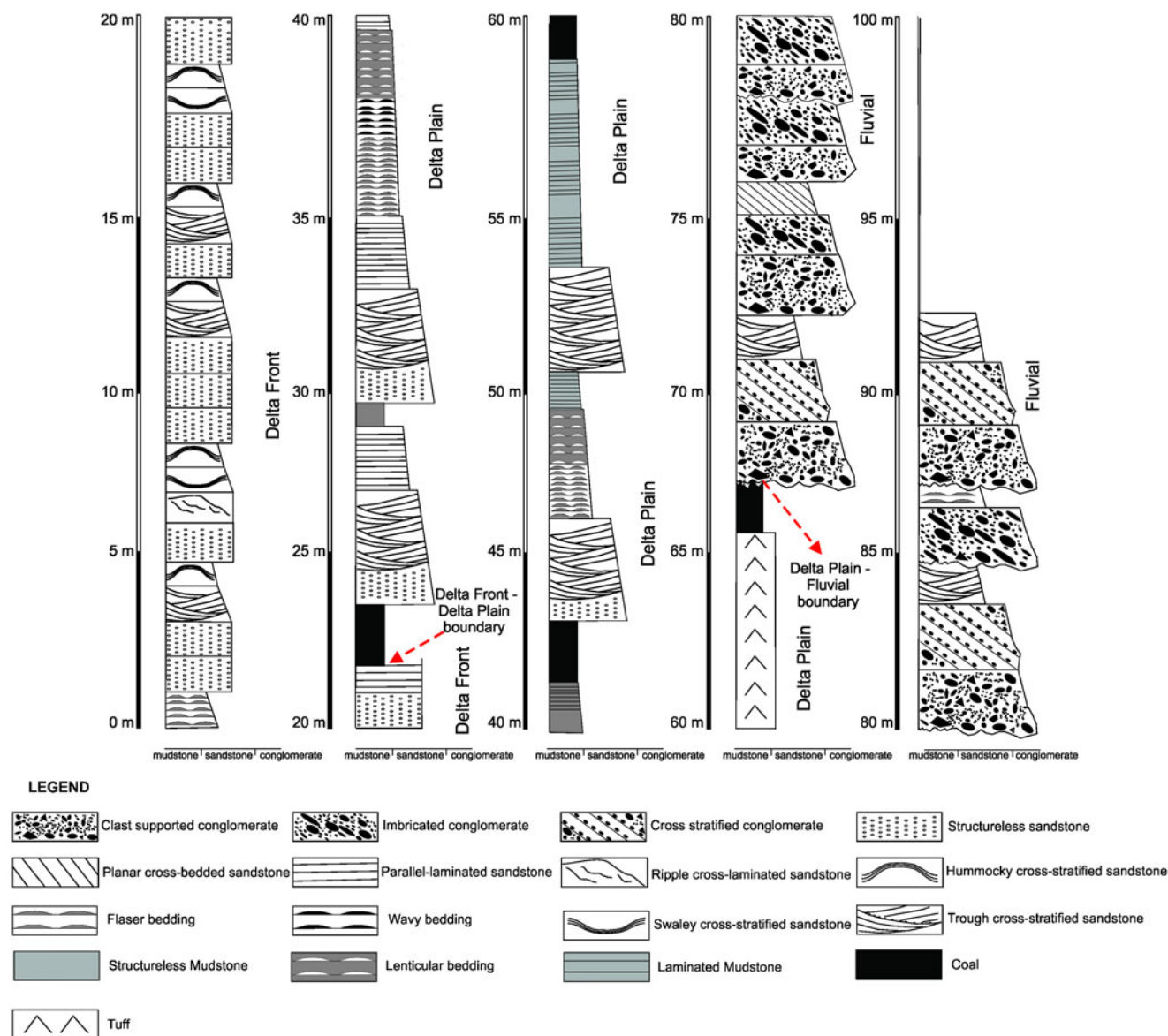


Fig. 17. Generalized stratigraphic column that illustrates the up-sequence evolution of the studied sedimentary succession. Note the shoaling-upward trend as documented by the transition of delta-front to tidally influenced delta-plain sediments and finally to fluvial deposits.

The tidal to fluvial transition in the Gauja Formation is gradual, with the development of fluvial channels with weak tidal influence that overlie delta-plain deposits. In contrast, in the NSB, delta-plain deposits are overlain by fluvial sediments with no evidence of tidal influence. This trend is interpreted as the result of the sudden increase in river power, associated with tectonic activity and large availability of coarse-grained sediment. This interpretation is compatible with the tectonic history of the NSB, indicating that it was influenced by the Hunter–Bowen Orogeny during the deposition of the sediments (Collins, 1991). Similarly, this trend has been observed in the Jurassic Lajas Formation, Argentina, and has been ascribed to high topographic gradients (Rossi & Steel, 2016).

The relative power of the tidal vs wave vs fluvial currents is the critical factor that controls the delta type (Davis & Hayes, 1984; Plink-Björklund, 2012). The documented upward switch from storm- and/or wave-influenced (delta-front, FA3) to strongly tidally influenced (delta-plain, FA2) sedimentation suggests tidal amplification. The amplification of tidal energy may be related

to tectonic, incisional and morphologic constraints (for recent reviews see Goodbred & Saito, 2012; Plink-Björklund, 2012). The tectonically active regime of the study region and the absence of evidence of incision (according to the criteria of Boyd *et al.* 2006) indicate that tectonic confinement controlled the power of tidal currents. The absence of tidal signatures in the delta-front sediments could indicate deposition on a steep delta-front slope, where tidal currents are not usually well developed (Goodbred & Saito, 2012).

The observed tidal reworking in the studied delta-plain deposits indicates that river power was not strong enough to entirely suppress the tidal current. With fluctuating fluvial input, the tidal effect is recorded as distinct intervals of tidally influenced sediments, with interbeds of thicker fluvial-dominated deposits. The upward decrease in the tidal impact on deposition could be related to regional topography and the long-term progradation of the delta (i.e. the studied sections become more distal relative to the shoreline in the younging direction). High topographic gradients have



Fig. 18. (Colour online) Outcrop photograph illustrating the stratigraphic evolution and the transition from deltaic to fluvial sedimentation in the NSB. (a) Bar Beach. (b) Merewether Beach. (c) Dudley North. (d) Dudley South. Note the presence of thick and laterally extensive volcanoclastic sediments (tuff) at the boundary between the underlying deltaic and the overlying fluvial deposits.

also been invoked to explain the limited landward penetration of the tidal currents into the fluvial realm in the Jurassic Lajas Formation, Argentina (Rossi & Steel, 2016). In addition, this trend in the NSB could be the result of local parameters (e.g. sideways limitations in distributary channel mouths) controlling the tidal reworking. Gradual prevalence of fluvial vs tidal processes has also been observed in the Baltic Basin (Tänavsuu-Milkeviciene & Plink-Björklund, 2009; Rossi & Steel, 2016). The sedimentary succession in the Baltic Basin portrays an upwards transition from a tide-dominated delta to a tidally influenced delta, because of the increasing contribution of the river system. The Campanian Chimney Rock Tongue, Western Interior Seaway of Wyoming–Utah, USA, serves as an example of the control of local parameters in the formation of tidally influenced facies (Plink-Björklund, 2008). In the Chimney Rock Tongue, tidally influenced facies are only recorded in the distributary channel mouths and within some mouth bars, and, in conjunction with the change in the style of mouth bars within the deltaic system, indicate that the tidal reworking was controlled by local conditions.

7.b. Sequence stratigraphy, and tectonic controls on sedimentation

Sequence stratigraphy is a powerful tool that aids in understanding the evolution of sedimentary basins (Cantalamessa *et al.* 2007;

Rodríguez-Tovar *et al.* 2007; Catuneanu *et al.* 2009, 2011; Di Celma *et al.* 2010; Zecchin *et al.* 2011; Eriksson *et al.* 2013; Maravelis *et al.* 2018) and also has valuable implications for the industry (De Gasperi & Catuneanu, 2014; Zecchin & Catuneanu, 2015). The interpretation of systems tracts relies on the observation of stratal stacking patterns, the nature of the bounding surfaces and the relationship with the adjacent stratigraphic units (Catuneanu, 2017).

The observed progradation and aggradation of the deltaic system suggest deposition during a normal regression of the shoreline. Normal regressions can be associated with either lowstand or highstand systems tracts (LST and HST respectively), and the lowstand vs highstand interpretation is most reliably based on the underlying stacking pattern: a normal regression that follows a forced regression belongs to the LST, whereas a normal regression that follows a transgression belongs to the HST (Catuneanu, 2017). In this case study, the underlying stacking pattern is not exposed. Further subsurface work is required for an unequivocal interpretation of systems tracts. However, the abrupt increase in grain size and energy levels across the subaerial unconformity, from the deltaic system to the overlying fluvial system, fits the common vertical trends of depositional sequences, where accumulation is typically accompanied by a decrease in energy levels and grain size from base to top. Consequently, the finer-grained deltaic system below the depositional sequence boundary can be interpreted as

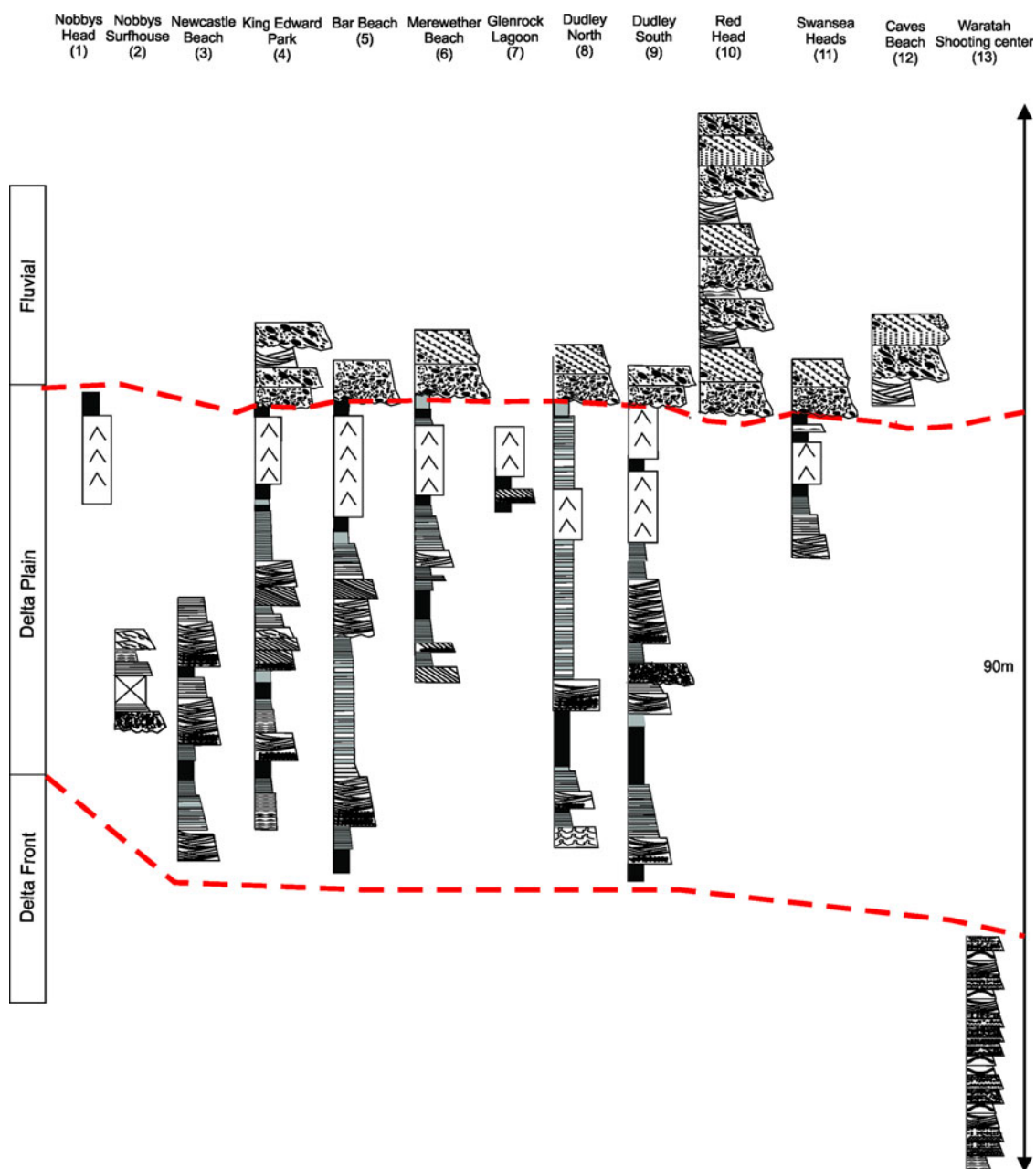


Fig. 19. (Colour online) Synthetic stratigraphic cross-section of the studied region that presents the spatial and temporal evolution of different depositional environments and sub-environments. Note the shoaling-upward trend as documented by the transition of delta-front to tidally influenced delta-plain sediments and finally to fluvial deposits. Red lines indicate interpreted boundaries between depositional settings. See Figure 9 for legend symbols.

a highstand systems tract, whereas the coarser-grained fluvial system above the depositional sequence boundary can be interpreted as a lowstand systems tract. Both lowstand and highstand systems tracts indicate deposition during relative sea-level rise, whereas the intervening subaerial unconformity is interpreted to have formed during a stage of relative sea-level fall.

The subaerial unconformity (SU) is typified by channelized truncations of the underlying deltaic deposits by fluvial erosion (Fig. 21). In this case, the fluvial system is not genetically related to the underlying deltaic system; i.e. they belong to different accommodation cycles. The delta-front deposits correspond to the foresets and the delta-plain deposits to the topsets of the HST. Given the progradation of the deltaic system, it is inferred that the delta-front sediments could overlie pro-delta deposits. In this scenario, these pro-delta

deposits would represent the bottom sets of the HST. Further subsurface work is required to establish the stacking pattern of the deposits that underlie the observed sections presented in this paper. This will afford a more precise reconstruction of the sequence-stratigraphic framework. The erosional character of the SU indicates reworking by the overlying high-energy fluvial system that belongs to the LST. This system is interpreted as the product of deposition in braided rivers and relates to the steepening of topographic gradients, which accompanied the uplift of the New England Orogen.

In an alternative sequence-stratigraphic interpretation, the delta front deposits (FA3) could be attributed to highstand (HST) and/or falling-stage (FSST) systems tracts, and the overlying delta plain sediments (FA2) to a lowstand (LST) systems tract. This interpretation could explain the switch from wave/storm- and river-influenced

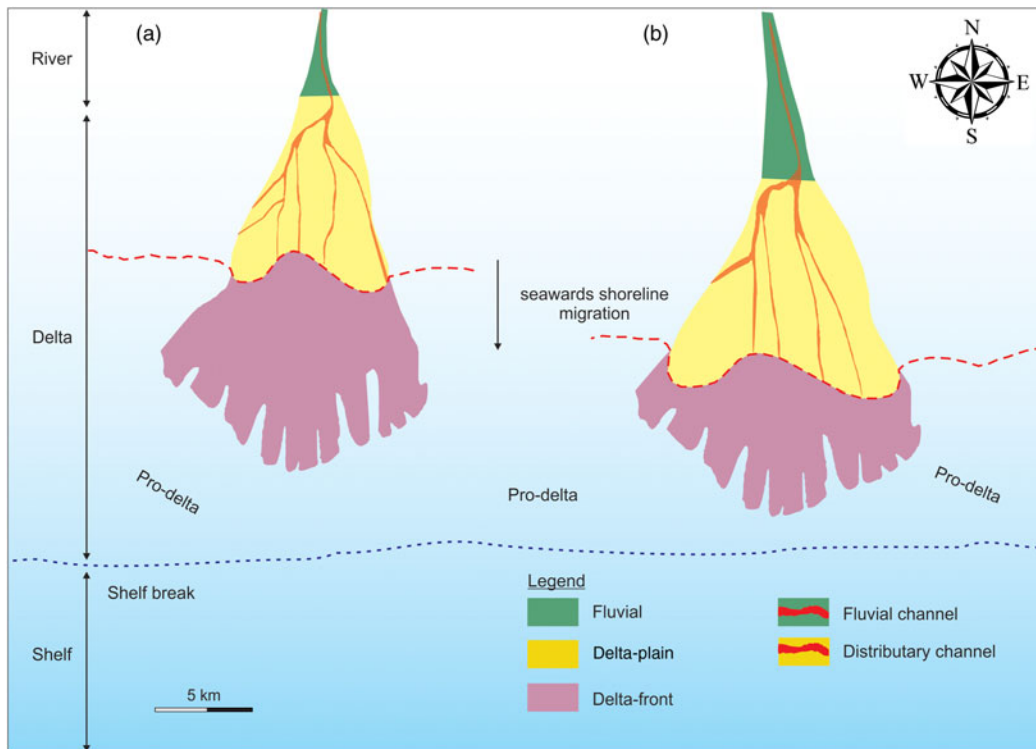


Fig. 20. (Colour online) Schematic block diagram that depicts the evolutionary stages of the deltaic system. Note the progradation of delta-plain deposits over the deeper-positioned delta-front deposits (modified from Chen *et al.* 2014).

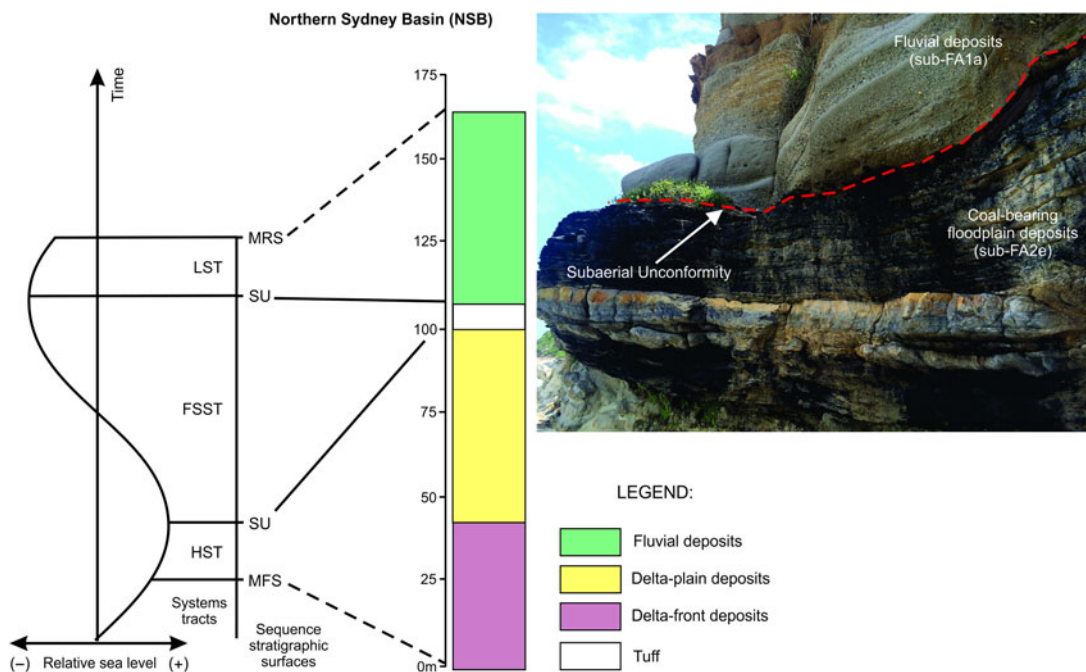


Fig. 21. (Colour online) Sequence-stratigraphic framework for the Northern Sydney Basin. Note the (1) long-term (second-order) shoaling-upward trend from delta-front to fluvial sediments, and (2) interpretation of the depositional facies in terms of third-order systems tracts. Dashed lines represent inferred sequence-stratigraphic surfaces; MFS = maximum flooding surface; MRS = maximum regressive surface; SU = subaerial unconformity; HST = highstand systems tract; LST = lowstand systems tract; FSST = falling stage systems tract.

sedimentation in the delta front to the tide-influenced sedimentation in the delta plain. However, this alternative interpretation would require another subaerial unconformity between the delta front (FA3) and the delta plain (FA2), which has not been observed

in the field. In the absence of field evidence to support a more complicated sequence-stratigraphic interpretation, the simpler interpretation is favoured in this paper, which assigns both FA3 and FA2 to one HST delta. The tidal amplification noted from

FA3 to FA2 can be attributed to various factors, including: (1) FA3 is only exposed at one outcrop, where no evidence of tidal currents has been observed; however, the potential tidal influence in FA3 cannot be ruled out; (2) 'hyper-synchronous' conditions (*sensu* Dalrymple & Choi, 2007) can explain an increase in the tidal range and current velocities from delta front to delta plain sub-environments (see also earlier discussion).

The grain size and nature (the relative contribution of rivers, waves/storms and tides) of the tidally influenced deltaic systems are associated with tectonic, sedimentary and topographic parameters that in turn control the sediment calibre and availability, as well as the effectiveness, of the depositional process. The studied succession offers a rare example of a sand-rich, regressive fluvio-deltaic system, developed adjacent to tectonically active mountains (New England Orogen). In contrast to most of the modern examples of such systems that are mud-rich (Rossi & Steel, 2016), the studied system is coarser-grained and dominated by gravel (FA1) and sand-rich deposits (FA2 and FA3). This could be associated with the proximity of the source area, and the possible steep gradients of the inherited topography. These features, in association with the abundance of coarse-grained sediment, could also explain the switch from storm-influenced (FA3) to tidally influenced (FA2) sedimentation, and the absence of landward penetration of the tidal currents into the fluvial realm. The Jurassic Lajas Formation, Argentina, offers another example of a sand-rich fluvio-deltaic system, with abrupt termination of tidal influence at the delta-plain/fluvial boundary. The development of this system has also been associated to the great proximity of the source region and the steep topographic gradients (Rossi & Steel, 2016). It is possible that the fluvio-deltaic system is larger, and that the systems recognized in the study area were in fact different distributary channels of the same river system, transformed by regional-scale tectonic elements.

The main regional tectonic element is the NW–SE-oriented Peel–Manning Fault (Collins, 1991, fig. 1). The Peel–Manning Fault System corresponds to a major arcuate zone that is composed of serpentinite and mylonite. The fault system extends northward beyond the Queensland border, where it is covered by Mesozoic sediments. This fault system has a complex tectonic history, possibly dating from the Cambrian, and has kinematic elements including thrust, dextral strike-slip and sinistral strike-slip. Most of the later movement is strike-slip (Offler & Hand, 1988), associated with E–W shortening during uplift of the New England Orogen (Collins, 1991). Major Permian movement on the Peel–Manning Fault System might be recorded by the 280–275 Ma (Lanphere & Hockley, 1976), whereas the youngest movement of the Peel–Manning Fault System is thought to take place at 248 Ma (Cooper *et al.* 1963). These geochronological constraints indicate that the Peel–Manning Fault System was active during the deposition of the studied succession. The entire orogenic cycle, starting with folding in the Middle to Late Permian and terminating with dispersal of tectonostratigraphic blocks in the Late Permian – Early Triassic (Collins, 1991), allowed a large amount of coarse-grained material, from the rapidly uplifting source area (New England Orogen), to be made available for sedimentation in the SB (the Permo-Triassic megacycle of Conaghan *et al.* 1982). The palaeocurrent indicators exhibit a SE- to SW-directed transport direction and indicate a NW- to NE-positioned sediment source (Fig. 20). These data suggest sediment transport directions that are either parallel or perpendicular to the Peel–Manning Fault System. In particular, the stratigraphically lower delta-plain deposits display a S, SE (axial) transport pathway, whereas the overlying

fluvial sediments exhibit a mostly SW (transverse) palaeoflow pattern. This axial transport could be related to the growth of a fluvio-deltaic drainage divide, probably controlled by surface uplift along the eastern edge of the Peel–Manning Fault System. The transverse-flowing systems are interpreted as fluvial transport transverse to the evolving deformation front. Similar features have been described in the Jurassic Lajas Formation, Argentina. The lowermost parts of the formation display a palaeoflow trend parallel to the fault and/or fold element that becomes perpendicular up-sequence, indicating the contribution of this tectonic element on the development of the depositional systems (Rossi & Steel, 2016).


8. Conclusions

This outcrop-based integrated investigation of facies, sequence-stratigraphic and palaeoflow analysis applied to the studied Upper Permian sedimentary succession provides valuable information about the syn-depositional conditions in the NSB, SE Australia, including: (1) the spatial and temporal distribution of the depositional environments; (2) the dominant physical processes of deposition; and (3) palaeoenvironmental evolution, as inferred from the observed sedimentologic and stratigraphic features.

- The studied succession includes 15 depositional facies (F1–F15) that are grouped into three facies associations (FA1–FA3). In addition, FA1 and FA2 are further subdivided into different sub-facies associations (sub-FA1a and sub-FA1b, and sub-FA2a to sub-FA2f). This grouping of facies and sub-facies associations reflects variations in the dominant physical process and represents delta-front, delta-plain and fluvial settings.
- The progradation and aggradation of the deltaic system is supported by the following evidence: (1) the depositional trend associated with an overall shallowing-upward succession; this succession evolves from delta-front to delta-plain deposits; (2) the coarsening-upward trend; (3) the architectural relations that document delta-plain distributary channel-fill successions dominated by lateral accretion elements, overlain by fluvial channels dominated by downcurrent accretion elements; and (4) the lack of any upward-deepening successions.
- The contribution of wave, tidal and fluvial currents is variable in the different environments and sub-environments. The delta-front deposits are wave/storm-influenced. The delta-plain sediments are influenced by tidal currents, but their deposition was mainly controlled by fluvial action. The delta-plain deposits record an upward increase in the fluvial energy, and an associated decrease in the frequency and diversity of sedimentary structures that indicate tidal influence. This may relate to an increase with time in (1) topographic gradients and fluvial energy, and/or (2) the distance between the location of the studied sections and the prograding shoreline. The overlying fluvial sediments are not affected by tides, and the river power is the dominant process that controls deposition. This upward decrease of wave and tidal reworking and the predominance of river processes can be ascribed to steep topographic gradients and large availability of coarse-grained sediment, as a result of uplift during active tectonism in the New England Orogen.
- The unconformable stratigraphic relationship of the fluvial sediments with the underlying deltaic deposits indicates that these units are not genetically related. The deltaic system is interpreted as the foreset (delta front) and the topset (delta plain) of a highstand systems tract, whereas the overlying fluvial

system is interpreted as the topset of a lowstand systems tract. Both systems tracts document deposition during relative sea-level rise. Their contact is a subaerial unconformity, interpreted to correspond to a period of relative sea-level fall in the NSB.

- Palaeocurrent data from different stratigraphic levels of the studied succession indicate a trend that is initially parallel to the main structural element (New England Orogen). Up-sequence, the palaeodispersal trend becomes perpendicular to the structural high, indicating an influence of this tectonic element on sedimentation.

Author ORCID.  Angelos G. Maravelis 0000-0002-9694-7500

Acknowledgements. This investigation was sponsored by the Geological Survey of New South Wales (GSNSW), through the research project 'Stratigraphic Correlation: Nobbys Tuff-Althorpe Claystone (Kevin Ruming)'. Bulga Coal is thanked for allowing access to the open cut pit and facilitating the collection of field data. The authors acknowledge the journal editor Stephen Hubbard, the journal reviewer Don I. Cummings and two anonymous reviewers for their constructive reviews that improved the manuscript. The authors thank Donatella Mellere for the thorough editing and valuable discussions that improved a previous draft of this research. Our colleagues Alexandra Scott and Sean Melehan are acknowledged for their valuable contribution during several field excursions.

References

- Alder JD, Hawley S, Maung T, Scott J, Shaw RD, Sinelnikov A and Kouzmina G (1998) Prospectivity of the offshore Sydney Basin: a new perspective. *Journal of the Australian Petroleum Exploration Association* **38**, 68–92.
- Alexander J and Fielding C (1997) Gravel antidunes in the tropical Burdekin River, Queensland, Australia. *Sedimentology* **44**, 327–37.
- Allen J (1983) Studies in fluvial sedimentation: bars, bar-complexes and sandstone sheets (low-sinuosity braided streams) in the brownstones (L. Devonian), Welsh borders. *Sedimentary Geology* **33**, 237–93.
- Ashworth PJ, Sambrook Smith GH, Best JL, Bridge JS, Lane SN, Lunt IA, Reesink AJH, Simpson CJ and Thomas RE (2011) Evolution and sedimentology of a channel fill in the sandy braided South Saskatchewan River and its comparison to the deposits of an adjacent compound bar. *Sedimentology* **58**, 1860–83.
- Bhattacharya JP and Willis BJ (2001) Lowstand deltas in the Frontier Formation, Powder River Basin, Wyoming: implications for sequence stratigraphic models, USA. *American Association of Petroleum Geologists Bulletin* **80**, 139–50.
- Boyd R, Dalrymple RW and Zaitlin BA (2006) Estuarine and incised-valley facies models. In *Facies Models Revisited* (eds HW Posamentier and RG Walker), pp. 171–235. Tulsa, Oklahoma: SEPM Special Publication no. 84.
- Bridge JS (2003) *Rivers and Floodplains: Forms, Processes, and Sedimentary Record*. Oxford: Blackwell.
- Bridge JS (2006) Fluvial facies models: recent developments. In *Facies Models Revisited* (eds H Posamentier and RG Walker), pp. 85–170. Tulsa, Oklahoma: SEPM Special Publication no. 84.
- Cant DJ and Walker RG (1978) Fluvial processes and facies sequences in the sandy braided South Saskatchewan River, Canada. *Sedimentology* **25**, 625–48.
- Cantalamesa G, Di Celma C, Ragaini L, Valleri G and Landini W (2007) Sedimentology and high-resolution sequence stratigraphy of the late middle to late Miocene Angostura Formation (western Borbón Basin, northwestern Ecuador). *Journal of the Geological Society of London* **164**, 653–65.
- Carvajal C and Steel R (2009) Shelf-edge architecture and bypass of sand to deep water: influence of shelf-edge processes, sea-level, and sediment supply. *Journal of Sedimentary Research* **79**, 652–72.
- Catuneanu O (2004) Basement control on flexural profiles and the distribution of foreland facies: the Dwyka Group of the Karoo Basin, South Africa. *Geology* **32**, 517–20.
- Catuneanu O (2006) *Principles of Sequence Stratigraphy*. Amsterdam: Elsevier. 375 pp.
- Catuneanu O (2017) Sequence stratigraphy: guidelines for a standard methodology. In *Stratigraphy and Timescales* (ed. M Montenari), pp. 1–57. Amsterdam: Academic Press.
- Catuneanu O and Eriksson PG (2002) Sequence stratigraphy of the Precambrian Rooihooft–Timeball Hill rift succession, Transvaal Basin, South Africa. *Sedimentary Geology* **147**, 71–88.
- Catuneanu O, Hancox PJ and Rubidge BS (1998) Reciprocal flexural behaviour and contrasting stratigraphies: a new basin development model for the Karoo retroarc foreland system, South Africa. *Basin Research* **10**, 417–39.
- Catuneanu O, Wopfner H, Eriksson PG, Cairncross B, Rubidge BS, Smith RMH and Hancox PJ (2005) The Karoo basins of south-central Africa. *Journal of African Earth Sciences* **43**, 211–53.
- Catuneanu O, Khalifa MA and Wanas HA (2006) Sequence stratigraphy of the Lower Cenomanian Bahariya Formation, Bahariya Oasis, Western Desert, Egypt. *Sedimentary Geology* **190**, 121–37.
- Catuneanu O, Abreu V, Bhattacharya JP, Blum MD, Dalrymple RW, Eriksson PG, Fielding CR, Fisher WL, Galloway WE, Gibling MR, Giles KA, Holbrook JM, Jordan R, Kendall CGSC, Macurda B, Martinsen OJ, Miall AD, Neal JE, Nummedal D, Pomar L, Posamentier HW, Pratt BR, Sarg JF, Shanley KW, Steel RJ, Strasser A, Tucker ME and Winker C (2009) Towards the standardization of sequence stratigraphy. *Earth Sciences Reviews* **92**, 1–33.
- Catuneanu O, Galloway WE, Kendall CGSC, Miall AD, Posamentier HW, Strasser A and Tucker ME (2011) Sequence stratigraphy: methodology and nomenclature. *Newsletters in Stratigraphy* **44**, 173–245.
- Chen S, Steel RJ, Dixon JF and Osman A (2014) Facies and architecture of a tide-dominated segment of the Late Pliocene Orinoco Delta (Morne L'Enfer Formation) SW Trinidad. *Marine and Petroleum Geology* **57**, 208–32.
- Collins W (1991) A reassessment of the 'Hunter-Bowen Orogeny': tectonic implications for the southern New England fold belt. *Australian Journal of Earth Sciences* **38**, 409–23.
- Collinson JD (1996) Alluvial sediments. In *Sedimentary Environments: Processes, Facies and Stratigraphy* (ed. HD Reading), pp. 37–82. Oxford: Blackwell Publishing.
- Collinson JD, Mountney NP and Thompson DB (2006) *Sedimentary Structures*, 3rd edn. Harpenden: Terra Publishing.
- Conaghan PJ, Jones JG, McDonnell KL and Rouce K (1982) A dynamic fluvial model for the Sydney Basin. *Journal of the Geological Society of Australia* **29**, 55–70.
- Cooper JA, Richards JR and Webb AW (1963) Some potassium-argon ages in New England, New South Wales. *Journal of the Geological Society of Australia* **10**, 313–16.
- Cummings DI, Arnott RW and Hart BS (2006) Tidal signatures in a shelf-margin delta. *Geology* **34**, 249–52.
- Cummings DI, Dumas S, and Dalrymple RW (2009) Fine-grained versus coarse-grained wave ripples generated experimentally under largescale oscillatory flow. *Journal of Sedimentary Research* **79**, 83–93.
- Daidu F (2013) Classifications, sedimentary features and facies associations of tidal flats. *Journal of Paleogeography* **2**, 66–80.
- Dalrymple RW (2010) Tidal depositional systems. In *Facies Models 4*. (eds NP James and RW Dalrymple), pp. 201–32. St. John's, Geological Association of Canada.
- Dalrymple RW and Choi K (2007) Morphologic and facies trends through the fluvial–marine transition in tide-dominated depositional systems: a schematic framework for environmental and sequence-stratigraphic interpretation. *Earth Science Reviews* **81**, 135–74.
- Dalrymple RW, Zaitlin BA and Boyd R (1992) Estuarine facies models: conceptual basis and stratigraphic implications. *Journal of Sedimentary Petrology* **62**, 1130–1146.
- Davies R, Howell J, Boyd R, Flint S and Diessel C (2006) High-resolution sequence stratigraphic correlation between shallow-marine and terrestrial strata: examples from the Sunnyside Member of the Cretaceous Blackhawk Formation, Book Cliffs, eastern Utah. *American Association of Petroleum Geologists Bulletin* **90**, 1121–40.
- Davis RA and Hayes MO (1984) What is a wave-dominated coast? In *Hydrodynamics and Sedimentation in Wave-Dominated Coastal Environments* (eds B Greenwood and RA Davis Jr), pp. 313–29. Amsterdam: Marine Geology. vol. 60.

- De Gasperi A and Catuneanu O** (2014) Sequence stratigraphy of the Eocene turbidite reservoirs in Albacora field, Campos Basin, offshore Brazil. *American Association of Petroleum Geologists Bulletin* **98**, 279–313.
- De Raaf JFM, Boersma JR and Van Gelder A** (1977) Wave generated structures and sequences from a shallow marine succession, Lower Carboniferous, County Cork, Ireland. *Sedimentology* **4**, 1–52.
- Di Celma C, Cantalamessa G, Landini W and Ragaini L** (2010) Stratigraphic evolution from shoreface to shelf-indenting channel depositional systems during transgression: insights from the lower Pliocene Súa Member of the basal Upper Onzole Formation, Borbón Basin, northwest Ecuador. *Sedimentary Geology* **223**, 162–79.
- Diessel CFK** (1992) *Coal-Bearing Depositional Systems*. Berlin: Springer-Verlag, 721 pp.
- Diessel CFK and Warbrooke PR** (1987) The depositional environment of the Waratah Sandstone and the Borehole Seam. *21st Symposium Guide*. University of Newcastle Publication no. 273, 20 pp.
- Dumas S and Arnott RWC** (2006) Origin of hummocky and swaley cross-stratification: the controlling influence of unidirectional current strength and aggradation. *Geology* **34**, 1073–6.
- Eriksson PG, Banerjee S, Catuneanu O, Corcoran PL, Eriksson KA, Hiatt EE, Laflamme M, Lenhardt N, Long DG F, Miall AD, Mints MV, Pufahl PK, Sarkar S, Simpson EL and Williams GE** (2013) Secular changes in sedimentation systems and sequence stratigraphy. *Gondwana Research* **24**, 468–89.
- Ethridge FG, Skelly RL and Bristow CS** (1999) Avulsion and crevasing in the sandy braided Niobrara River: complex response to base-level rise and aggradation. In *Fluvial Sedimentology VI* (eds J Rogers and J Smith), pp. 179–91. Oxford: Blackwell. International Association of Sedimentologists Special Publication no. 28.
- Friend P, Hirst J and Nichols G** (1986) Sandstone-body structure and river process in the Ebro Basin of Aragon, Spain. *Caudernos Geologia Iberica* **10**, 9–30.
- Glen RA** (2005) The Tasmanides of eastern Australia. In *Terrane Processes at the Margins of Gondwana* (eds APM Vaughan, PT Leat and RJ Pankhurst), pp. 23–96. Geological Society of London, Special Publication no 246.
- Glen RA and Beckett J** (1997) Structure and tectonics along the inner edge of a foreland basin: the Hunter Coalfield in the northern Sydney Basin, New South Wales. *Australian Journal of Earth Sciences* **44**, 853–77.
- Goodbred SLJR and Saito Y** (2012) Tide-dominated deltas. In *Principles of Tidal Sedimentology* (eds RA Davis and RW Dalrymple), pp. 129–49. Springer: Berlin.
- Guion PD, Fulton IM and Jones NS** (1995) Sedimentary facies of the coal-bearing Westphalian A and B north of the Wales-Sbrabant High. In *European Coal Geology* (eds MKG Whateley and DA Spears), pp. 45–78. Geological Society of London, Special Publication no 82.
- Herbert C** (1995) Sequence stratigraphy of the Late Permian Coal Measures in the Sydney Basin. *Australian Journal of Earth Sciences* **42**, 391–405.
- Herbert C** (1997) Relative sea level control of deposition in the Late Permian Newcastle Coal Measures of the Sydney Basin, Australia. *Sedimentary Geology* **107**, 167–87.
- Herbert C and Helby R** (1980) A guide to the Sydney Basin. *Geological Survey of New South Wales Bulletin* **26**, 603.
- Ichaso AA and Dalrymple RW** (2014) Eustatic, tectonic and climatic controls on an early synrift mixed-energy delta, Tilje Formation (early Jurassic, Smørbukk Field, offshore mid-Norway). In *Depositional Systems to Sedimentary Successions on the Norwegian Continental Shelf* (eds AW Martinus, R Ravnas, JA HowellRJ Steel and JP Wonham), pp. 339–88. Oxford: Blackwell. International Association of Sedimentologists Special Publication no. 46.
- Jenkins RB, Landenberger B and Collins WJ** (2002) Late Palaeozoic retreating and advancing subduction boundary in the New England Fold Belt, New South Wales. *Australian Journal of Earth Sciences* **49**, 467–89.
- Jenkins RB and Offler R** (1996) Metamorphism and deformation of an Early Permian extensional basin sequence: the Manning Group, southern New England Orogen. *Australian Journal of Earth Sciences* **43**, 423–36.
- Landenberger B, Farrell TR, Offler R, Collins WJ and Whitford DJ** (1995) Tectonic implications of Rb-Sr biotite ages for the Hillgrove Plutonic Suite, New England Fold Belt, N.S.W., Australia. *Precambrian Research* **71**, 251–63.
- Lanphere MA and Hockley JJ** (1976) The age of nephrite occurrences in the Great Serpentine Belt of New South Wales. *Journal of the Geological Society of Australia* **23**, 15–17.
- Leckie DA** (1988) Wave-formed, coarse-grained ripples and their relationship to hummocky cross-stratification. *Journal of Sedimentary Petrology* **58**, 607–22.
- Leckie DA and Walker RG** (1982) Storm and tide dominated shorelines in Late Cretaceous Moosebar-Lower Gates Interval – outcrop equivalents of deep basin gas traps in western Canada. *American Association of Petroleum Geologists Bulletin* **66**, 138–57.
- Legler B, Johnson HD, Hampson GJ, Massart BYG, Jackson CA-L, Jackson MD, El-Barkooky A and Ravnas R** (2013) Facies model of a fine-grained, tide-dominated delta: Lower Dir Abu Lifa Member (Eocene), Western Desert, Egypt. *Sedimentology* **60**, 1313–56.
- Longhitano SG, Mellere D, Steel RJ and Ainsworth RB** (2012) Tidal depositional systems in the rock record: a review and new insights. *Sedimentary Geology* **279**, 2–22.
- Lowe DR** (1988) Suspended-load fallout rate as an independent variable in the analysis of current structures. *Sedimentology* **35**, 765–76.
- MacEachern JA and Bann KL** (2008) The role of ichnology in refining shallow marine facies models. In *Recent Advances in Models of Siliciclastic Shallow-Marine Stratigraphy* (eds GJ Hampson, RJ Steel, PM Burgess and RW Dalrymple), pp. 73–116. Tulsa, Oklahoma: SEPM Special Publication no. 90.
- Magalhães AJC, Scherer CMS, Raja Gabaglia GP, Ballico MB and Catuneanu O** (2014) Unincised fluvial and tide-dominated estuarine systems from the Mesoproterozoic Lower Tombador Formation, Chapada Diamantina basin, Brazil. *Journal of South American Earth Sciences* **56**, 68–90.
- Magalhães AJC, Scherer CMS, Raja Gabaglia GP and Catuneanu O** (2015) Mesoproterozoic delta systems of the Açuruá Formation, Chapada Diamantina, Brazil. *Precambrian Research* **257**, 1–21.
- Maravelis A, Konstantopoulos P, Pantopoulos G and Zelilidis A** (2007) North Aegean sedimentary basin evolution during the Late Eocene to Early Oligocene based on sedimentological studies on Lemnos Island (NE Greece). *Geologica Carpathica* **58**, 455–64.
- Maravelis A and Zelilidis A** (2011) Geometry and sequence stratigraphy of the Late Eocene–Early Oligocene shelf and basin floor to slope turbidite systems, Lemnos Island, NE Greece. *Stratigraphy and Geological Correlation* **19**, 205–20.
- Maravelis AG, Boutelier D, Catuneanu O, Seymour KS and Zelilidis A** (2016) A review of tectonics and sedimentation in a forearc setting: Hellenic Thrace Basin, north Aegean Sea and northern Greece. *Tectonophysics* **674**, 1–19.
- Maravelis AG, Chamilaki E, Pasadakis N, Zelilidis A and Collins WJ** (2017a) Hydrocarbon generation potential of a Lower Permian sedimentary succession (Mount Agony Formation): Southern Sydney Basin, New South Wales, Southeast Australia. *International Journal of Coal Geology* **183**, 52–64.
- Maravelis AG, Chamilaki E, Pasadakis N, Vassiliou A and Zelilidis A** (2017b) Organic geochemical characteristics and paleodepositional conditions of an Upper Carboniferous mud-rich succession (Yagon Siltstone): Myall Trough, southeast Australia. *Journal of Petroleum Science and Engineering* **158**, 322–35.
- Maravelis AG, Catuneanu O, Nordsvan A, Landenberger B and Zelilidis A** (2018) Interplay of tectonism and eustasy during the Early Permian icehouse: Southern Sydney Basin, southeast Australia. *Geological Journal* **53**, 1372–403.
- Martin AJ** (2000) Flaser and wavy bedding in ephemeral streams: a recent and an ancient example. *Sedimentary Geology* **136**, 1–5.
- Martin MA, Wakefield M, MacPhail MK, Pearce T and Edwards HE** (2013) Sedimentology and stratigraphy of an intra-cratonic basin coal seam gas play: Walloon Subgroup of the Surat Basin, eastern Australia. *Petroleum Geoscience* **19**, 21–38.
- Martinus AW and Van den Berg JH** (2011) *Atlas of Sedimentary Structures in Estuarine and Tidally-Influenced River Deposits of the Rhine-Meuse-Scheldt System*. Houten: EAGE Publications.
- Martinus AW, Kaas I, Naess A, Helgesen G, Kjaereford JM and Keith DA** (2001) Sedimentology of heterolithic and tide-dominated Tilje Formation (Early Jurassic, Halten Terrace, offshore mid-Norway). In *Sedimentary Environments Offshore Norway – Paleozoic to Recent* (eds OJ Martinsen

- and T Dreyer), pp. 103–44. Stavanger: Norwegian Petroleum Foundation Special Publication no. 10.
- McIlroy D, Flint SS, Howell JA and Timms N** (2005) Sedimentology of the tide-dominated Jurassic Lajas Formation, Neuquen Basin, Argentina. In *The Neuquén Basin, Argentina: A Case Study in Sequence Stratigraphy and Basin Dynamics* (eds GD Veiga, LA Spalletti, JA Howell and E Schwarz), pp. 83–107. Geological Society of London, Special Publication no. 252.
- Medici G, Boulestei K, Mountney NP, West LJ and Odling NE** (2015) Palaeoenvironment of braided fluvial systems in different tectonic realms of the Triassic Sherwood Sandstone Group, UK. *Sedimentary Geology* **329**, 188–210.
- Mellere D and Steel RJ** (1995) Facies architecture and sequentiality of near-shore and shelf sandbodies; Haystack Mountains Formation, Wyoming, USA. *Sedimentology* **42**, 551–74.
- Mellere D and Steel RJ** (1996) Tidal sedimentation in inner Hebrides Half grabens, Scotland. In *The Mid-Jurassic Bearraig Sandstone Formation. Geology of Siliciclastic Shelf Seas* (eds D De Baptist and P Jacobs), pp. 49–79. Geological Society of London, Special Publication no. 117.
- Mellere D and Steel RJ** (2000) Style contrast between forced regressive and low-stand/transgressive wedges in the Campanian of south-central Wyoming (Hatfield Member of the Haystack Mountains Formation). In *Sedimentary Responses to Forced Regressions* (eds D Hunt and RL Gawthorpe), pp. 141–62. Geological Society of London, Special Publication no. 172.
- Mellere D, Mannie A, Longhitano S, Mazur M, Kulausa H, Brough S and Cotton J** (2016) Tidally influenced shoal water delta and estuary in the Middle Jurassic of the Søgne Basin, Norwegian North Sea: sedimentary response to rift initiation and salt tectonics. In *Sedimentology of Paralic Reservoirs: Recent Advances* (eds GJ Hampson, AD Reynolds, B Kostic and MR Wells). Geological Society of London, Special Publication no. 444.
- Menegazzo M, Catuneanu O and Chang HK** (2016) The South American retroarc foreland system: the development of the Bauru Basin in the back-bulge province. *Marine and Petroleum Geology* **73**, 131–56.
- Metcalfe I, Crowley JL, Nicoll RS and Schmitz M** (2015) High-precision U-Pb CA-TIMS calibration of Middle Permian to Lower Triassic sequences, mass extinction and extreme climate-change in eastern Australian Gondwana. *Gondwana Research* **28**, 61–81.
- Miall AD** (1977) A review of the braided-river depositional environment. *Earth-Science Reviews* **13**, 1–62.
- Miall AD** (1988) Architectural elements and bounding surfaces in fluvial deposits: anatomy of the Kayenta Formation (Lower Jurassic), Southwest Colorado. *Sedimentary Geology* **55**, 233–62.
- Miall AD** (1996) *The Geology of Fluvial Deposits, Sedimentary Facies, Basin Analysis and Petroleum Geology*. Berlin: Springer.
- Miall AD** (2014) *Fluvial Depositional Systems*. Berlin: Springer.
- Mohrig D, Heller P, Paola C and Lyons W** (2000) Interpreting avulsion process from ancient alluvial sequences: Guadalupe-Matarranya system (northern Spain) and Wasatch Formation (western Colorado). *Geological Society of America Bulletin* **112**, 1787–803.
- Montoya D** (2012) *Coal Seam Gas Royalties in Australian States & Territories*. Sydney, New South Wales (E-brief): NSW Parliament.
- Moretti M, Soria J, Alfaro P and Walsh N** (2001) Asymmetrical soft-sediment deformation structures triggered by rapid sedimentation in turbiditic deposits (Late Miocene, Guadix Basin, southern Spain). *Facies* **44**, 283–94.
- Myrow PM and Southard JB** (1991) Combined-flow model for vertical stratification sequences in shallow marine storm-deposited beds. *Journal of Sedimentary Petrology* **61**, 202–10.
- Nemec W and Steel R** (1984) Alluvial and coastal conglomerates: their significant features and some comments on gravelly mass-flow deposits. In *Sedimentology of Gravels and Conglomerates* (eds EH Koster and RJ Steel), pp. 1–31. Calgary, Alberta: Canadian Society of Petroleum Geologists Memoir no. 10.
- Nichols G** (1999) *Sedimentology and Stratigraphy*. Oxford: Blackwell Science.
- Nichols G and Fisher JA** (2007) Processes, facies and architecture of fluvial distributary system deposits. *Sedimentary Geology* **195**, 75–90.
- Nio SD and Yang CS** (1991) Sea-level fluctuations and geometric variability of tide-dominated sandbodies. *Sedimentary Geology* **70**, 161–93.
- O'Brien PE and Wells AT** (1986) A small, alluvial crevasse splay. *SEPM Journal of Sedimentary Research* **56**, 876–79.
- Offler R and Hand M** (1988) Metamorphism in the fore arc and subduction complex sequences of the southern New England Fold Belt. In *New England Orogen: Tectonics and Metallogenesis* (ed. JD Kleeman), pp. 78–86. Armidale: Department of Geology & Geophysics, University of New England.
- Palozzi J, Pantopoulos G, Maravelis AG, Nordsvan A and Zelilidis A** (2018) Sedimentological analysis and bed thickness statistics from a Carboniferous deep-water channel-levee complex: Myall Trough, SE Australia. *Sedimentary Geology* **364**, 160–79.
- Pemberton GS, Spila M, Pulham AJ, Saunders T, MacEachern JA, Robbins D and Sinclair IK** (2002) Ichnology and sedimentology of shallow marine to marginal marine systems: Ben Nevis and Avalon Reservoirs, Jeanne d'Arc Basin. *Geological Association of Canada, Short Course Notes* **15**, 343.
- Plink-Björklund P** (2005) Stacked fluvial and tide-dominated estuarine deposits in high-frequency (fourth-order) sequences of the Eocene Central Basin, Spitsbergen. *Sedimentology* **52**, 391–428.
- Plink-Björklund P** (2008) Wave-to-tide facies change in a Campanian shoreline complex, Chimney Rock Tongue, Wyoming-Utah, USA. In *Recent Advances in Models of Siliciclastic Shallow-Marine Stratigraphy* (eds G Hampson, R Steel, P Burgess and RW Dalrymple), pp. 265–91. Tulsa, Oklahoma: Society for Sedimentary Geology, Special Publication no. 90.
- Plink-Björklund P** (2012) Effects of tides on deltaic deposition: causes and responses. *Sedimentary Geology* **279**, 107–33.
- Pontén A and Plink-Björklund P** (2007) Depositional environments in an extensive tide-influenced delta plain, Middle Devonian Gauja Formation, Devonian Baltic Basin. *Sedimentology* **54**, 969–1006.
- Pontén A and Plink-Björklund P** (2009) Regressive to transgressive transits reflected in tidal bars, Middle Devonian Baltic Basin. *Sedimentary Geology* **218**, 48–60.
- Porebski SJ and Steel RJ** (2006) Deltas and sea-level change. *Journal of Sedimentary Research* **76**, 390–403.
- Rebata H, Räsänen ME, Gingras MK, Vieira V Jr., Barberi M and Irion G** (2006) Sedimentology and ichnology of tide-influenced Late Miocene successions in Western Amazonia: the gradational transition between the Pebas and Nauta formations. In *New Contributions on Neogene Geography and Depositional Environments in Amazonia* (eds C Hoorn and H Vohnhof), pp. 96–119. Amsterdam: Elsevier. *Journal of South American Earth Sciences* no. 21.
- Reineck HE and Wunderlich F** (1968) Classification and origin of flaser and lenticular bedding. *Sedimentology* **11**, 99–104.
- Roberts J and Engel BA** (1987) Depositional and tectonic history of the southern New England Orogen. *Australian Journal of Earth Sciences* **34**, 1–20.
- Rodríguez-Tovar FJ, Pérez-Valera F and Pèez-López A** (2007) Ichnological analysis in high resolution sequence stratigraphy: the Glossifungites ichnofacies in Triassic successions from the Betic Cordillera (southern Spain). *Sedimentary Geology* **198**, 293–307.
- Røe S-L and Hermansen M** (2006) New aspects of deformed cross-strata in fluvial sandstones: examples from Neoproterozoic formations in northern Norway. *Sedimentary Geology* **186**, 283–93.
- Rossi VM and Steel RJ** (2016) The role of tidal, wave and river currents in the evolution of mixed-energy deltas: example from the Lajas Formation (Argentina). *Sedimentology* **63**, 824–64.
- Rubidge BS, Hancox PJ and Catuneanu O** (2000) Sequence analysis of the Ecca-Beaufort contact in the southern Karoo of South Africa. *South African Journal of Geology* **103**, 81–96.
- Santos MGM, Almeida RP, Godinho LPS, Marconato A and Mountney NP** (2014) Distinct styles of fluvial deposition in a Cambrian rift basin. *Sedimentology* **61**, 881–914.
- Schwartz TM and Graham SA** (2015) Stratigraphic architecture of a tide-influenced shelf-edge delta, Upper Cretaceous Dorotea Formation, Magallanes Austral Basin, Patagonia. *Sedimentology* **62**, 1039–77.
- Stear WM** (1978) Sedimentary structures related to fluctuating hydrodynamic conditions in flood plain deposits of the Beaufort Group near Beaufort West, Cape. *Transactions of the Geological Society of South Africa* **81**, 393–9.
- Steel RJ and Thompson DB** (1983) Structures and textures in the Triassic braided stream conglomerates ('Bunter' Pebble Beds) in the Sherwood Sandstone Group, North Staffordshire, England. *Sedimentology* **30**, 341–67.

- Stewart R and Adler D** (eds) (1995) New South Wales petroleum potential. *Coal and Petroleum Geology Branch Bulletin* **1**, 5–36. Sydney: New South Wales Department of Mineral Resources.
- Tänavsuu-Milkeviciene K and Plink-Björklund P** (2009) Recognizing tide-dominated versus tide-influenced deltas: middle Devonian strata of the Baltic Basin. *Journal of Sedimentary Research* **79**, 887–905.
- Veevers JJ and Powell CM** (1987) Late Paleozoic glacial episodes in Gondwanaland reflected in transgressive–regressive depositional sequences in Euramerica. *Geological Society of America Bulletin* **98**, 475–87.
- Veevers JJ and Powell C** (eds) (1994) *Permian-Triassic Pangean Basins and Fold Belts along the Panthalassan Margin of Gondwanaland*. Boulder, Colorado: *Geological Society of America Memoir*, no 184. 368 pp.
- Visser MJ** (1980) Neap-spring cycles reflected in Holocene subtidal large-scale bedform deposits: a preliminary note. *Geology* **8**, 543–6.
- Wakefield OJW, Hougha E and Peatfield AW** (2015) Architectural analysis of a Triassic fluvial system: the Sherwood Sandstone of the East Midlands Shelf, UK. *Sedimentary Geology* **327**, 1–13.
- Whiting PJ, Dietrich WE, Leopold LB, Drake TG and Shreve RL** (1988) Bedload sheets in heterogeneous sediment. *Geology* **16**, 105–8.
- Willis BJ** (2005) Deposits of tide-influenced river deltas. In *River Deltas: Concepts, Models, and Examples* (eds L Giosan and JP Bhattacharya), pp. 87–129. Tulsa, Oklahoma: SEPM Special Publication no. 83.
- Willis BJ, Bhattacharya JP, Gabel SL and White CD** (1999) Architecture of a tide-influenced delta in the Frontier Formation of central Wyoming. *Sedimentology* **46**, 667–88.
- Willis BJ and Gabel SL** (2001) Sharp-based, tide-dominated deltas of the Sego sandstone, Book Cliffs, Utah, USA. *Sedimentology* **46**, 479–506.
- Willis BJ and Gabel SL** (2003) Formation of deep incisions into tide-dominated river deltas: implications for the stratigraphy of the Sego Sandstone, Book Cliffs, Utah, USA. *Journal of Sedimentary Research* **73**, 246–63.
- Yoshida S, Steel RJ and Dalrymple RW** (2007) Changes in depositional processes – an ingredient in a new generation of sequence-stratigraphic models. *Journal of Sedimentary Research* **77**, 447–60.
- Zecchin M and Catuneanu O** (2015) High-resolution sequence stratigraphy of clastic shelves III: applications to reservoir geology. *Marine and Petroleum Geology* **62**, 161–75.
- Zecchin M, Civile D, Caffau M, Sturiale G and Roda C** (2011) Sequence stratigraphy in the context of rapid regional uplift and high-amplitude glacio-eustatic changes: the Pleistocene Cutro Terrace (Calabria, southern Italy). *Sedimentology* **58**, 442–77.
- Zelilidis A and Kontopoulos N** (1999) Plio-Pleistocene alluvial architecture in marginal extensional narrow sub-basins: examples from southwest Greece. *Geological Magazine* **136**, 241–62.